FEMS Microbiology Ecology

Bacterial and fungal communities in sub-Arctic tundra heaths are shaped by contrasting snow accumulation and nutrient availability

Minna K. Männistö[1], Saija H. K. Ahonen [2], Lars Ganzert[1,3], Marja Tiirola[4], Sari Stark[5] and Max M. Häggblom[1,6]

[1] Natural Resources Institute Finland, Ounasjoentie 6, FI-96200 Rovaniemi, Finland

[2] Ecology and Genetics Research Unit, University of Oulu, P.O. Box 8000, FI-90014 Oulu, Finland

[3] Plankton and Microbial Ecology, Leibniz Institute of Freshwater Ecology and Inland Fisheries, Zur alten Fischerhütte 2, 16775 Stechlin, Germany

[4] Department of Biological and Environmental Science, Nanoscience Center, University of Jyväskylä, FI-40014 Jyväskylä, Finland

[5] Arctic Centre, University of Lapland, P.O. Box 122, FI-96101, Rovaniemi, Finland

[6] Department of Biochemistry and Microbiology, Rutgers University, 76 Lipman Drive, New Brunswick, NJ 08901, U.S.A.

[*]Corresponding author:

Minna Männistö
Natural Resources Institute Finland
Ounasjoentie 6
FI-96200 Rovaniemi, Finland
Tel. +358295325564
email minna.mannisto@luke.fi

Key words: bacterial community, fungal community, tundra, winter, climate change, snow

Abstract

Climate change is affecting winter snow conditions significantly in northern ecosystems but the effects of the changing conditions for soil microbial communities are not well understood. We utilized naturally occurring differences in snow accumulation to understand how the wintertime subnivean conditions shape bacterial and fungal communities in dwarf shrub-dominated sub-Arctic Fennoscandian tundra sampled in mid-winter, early and late growing season. Phospholipid fatty acid (PLFA) and qPCR analyses indicated that fungal abundance was higher in windswept tundra heaths with low snow accumulation and lower nutrient availability. This was associated with clear differences in the microbial community structure throughout the season. Members of *Clavaria* spp. and *Sebacinales* were especially dominant in the windswept heaths. Bacterial biomass proxies were higher in the snow-accumulating tundra heaths in the late growing season but there were only minor differences in the biomass or community structure in winter. Bacterial communities were dominated by members of Alphaproteobacteria, Actinomycetota and Acidobacteriota and were less affected by the snow conditions than the fungal communities. The results suggest that small-scale spatial patterns in snow accumulation leading to a mosaic of differing tundra heath vegetation shapes bacterial and fungal communities as well as soil carbon and nutrient availability.

Introduction

High-latitude soils store approximately half of the global soil organic carbon and hence it is of major concern how global climate change will affect decomposition rates and C flux to the atmosphere in these regions (Tarnocai et al. 2009, Schuur et al. 2015). Arctic regions are warming up to four times faster than the global average (Rantanen et al. 2022), with the cold season months warming at a much faster rate than the growing season (Mikkonen et al. 2015; Rantanen et al. 2022). In northern Fennoscandia, in addition to increasing winter month temperatures, the number of frost days has declined, exceptionally cold winter days have decreased, while exceptionally warm days and the number of freeze-thaw cycles have increased (Mikkonen et al. 2015; Kivinen et al. 2017; Lepy and Pasanen 2017). Precipitation is also increasing in high-latitude ecosystems (Groisman et al. 2005; McCrystall et al. 2021) which influences the amount of snow that accumulates during winter. The depth and insulating properties of the snowpack, however, depend on the form of precipitation. As the extremely warm winter days are increasing in Arctic ecosystems it is predicted that the precipitation will be more and more in the form of rain instead of snow, and the thickness and timing of snowpack may be reduced (Bintanja and Andry 2017; McCrystall et al. 2021). Furthermore, increased winter thaw and rain on snow events diminish the insulating properties of snow (Serreze et al. 2021) and may lead to colder soil temperatures during winter (Groffman et al. 2001). In addition to direct changes in precipitation and soil temperature, climate warming is altering wintertime soil temperature regimes also indirectly through changes in the dominant vegetation. Tundra ecosystems are undergoing strong expansion and increase of shrubs (Sturm et al. 2001b), which may control the winter-time soil temperatures by trapping more snow that leads to increased insulation (Sturm et al. 2001a). Due to the complex ways by which climate change is altering snow cover, there is a high need to better understand the role of snow cover for/on soil microbial communities.

The wintertime microbial activity contributes to a significant part of annual carbon cycling in tundra ecosystems (Oechel et al. 1997; Fahnestock et al. 1999; Euskirchen 2012; Natali et al. 2019), and in boreal and Arctic soils overwinter CO_2 effluxes may even exceed plant carbon uptake during the growing season (Natali et al. 2019). Microbial activity and CO_2 flux continue in tundra soils through the winter down to -20°C (Natali et al. 2019). In Fennoscandian tundra soil, bacterial activity down to -16°C was identified with stable isotope probing with distinct communities growing at different sub-zero temperatures (Gadkari et al. 2019). Around and below 0°C, soil microbial activities become, however, increasingly temperature sensitive (Mikan et al. 2002; Sullivan et al. 2008; Tilston et al. 2010), and microbial substrate utilization may shift to decomposition of more labile organic matter such as fresh litter and root exudates or microbial biomass and by-products further affecting the C and nutrient cycling (Mikan et al. 2002; Schimel et al. 2004; Grogan and Jonasson 2005; Sturm et al. 2005). Under a thick snow cover, soil temperatures are decoupled from air temperatures and may remain close to 0 °C throughout the coldest months (Schimel et al. 2004; Männistö et al. 2013; Pattison et al. 2014; Convey et al. 2018; Way and Lewkowicz, 2018; Rixen et al. 2022). Snow cover conditions thus control cold season microbial activities and deeper snow may enhance winter microbial respiration even to the degree that it switches the ecosystem annual net carbon exchange from a sink to source (Nobrega and Grogan 2007; Natali et al. 2019). However, increased cold season microbial respiration may have legacy effects to the following growing seasons. Snow manipulation experiments have indicated that increased microbial activity during winter may lead to depletion of labile C and over time to reduced growing season CO_2 emissions (Semenchuk et al. 2016; Sullivan et al 2020). Moreover, increased nitrogen (N) mineralization under deeper snow cover and associated higher soil temperatures may have significant consequences for plant growth and consequently carbon cycling especially in the nutrient limited tundra ecosystems (Schimel et al. 2004)

The current understanding of the effects of snow depth on soil microbial communities mainly derives from experimental manipulation of the snowpack. In subalpine grassland and temperate deciduous forest soils, strong changes were reported in the bacterial and fungal communities under reduced snow cover during winter, but these differences leveled out during the growing season (Aanderud et al. 2017; Gavazov et al. 2017). In boreal forest soil, no effect of snow depth or snow properties was detected in bacterial or fungal communities either before or after spring thaw or in the late growing season (Männistö et al. 2018). On the other hand, strong shifts were reported in microbial communities of alpine grasslands during spring thaw and these were linked to shifts in microbial functions and biogeochemical fluxes suggesting that changes in the timing of spring thaw may have important consequences for the ecosystem functioning (Broadbent et al. 2021). In acidic tundra soils, bacterial community structure was significantly affected by snow depth which was associated with changes in edaphic factors (Ricketts et al. 2016). Semenova et al. (2016) reported changes in the abundance and community structure of saprotrophic, ectomycorrhizal, plant pathogenic, lichen- and bryophyte-associated fungal guilds with deeper snow. These changes were not entirely associated with shifts in vegetation but there were indications that fungal communities in the Arctic may exhibit faster turnover which is influenced e.g. by soil nutrient availability and dynamics of other microbial groups. Experimental manipulations of snow cover conditions have shown both differing vegetation (Olofsson et al. 2009) and higher soil microbial N and bacterial counts (Buckeridge and Grogan 2010) with deepened snow. Together, these studies indicate that there may be large differences in the resilience and sensitivity of bacterial and fungal communities to changes in winter soil temperature and moisture in different soil ecosystems. In addition, experimental manipulations of snow depth are often of short duration and may thus not necessarily depict long-term changes that would be mediated by the combination of differing vegetation, nutrient availability, and temperature regimes, which all change in response to differing snow cover.

In tundra landscapes, the small-scale variation in topography, which in turn affects wintertime snow accumulation, leads to a mosaic of habitats with differing snow conditions and dominant vegetation over a gradient from low and absent snow cover to snow accumulating sites (Oksanen and Virtanen 1995, Niittynen et al. 2020). Exposed ridges that are windswept remain nearly snow-free throughout the winter, while sheltered slopes and depressions accumulate snow already early in winter that remains until early summer. The windswept (WS) and snow-accumulating (SA) habitats exhibit widely divergent winter-time soil temperatures and the duration of the snow-free period, which gives rise to divergent plant coverage, amount of litter and nutrient availability (Niittynen et al. 2020). In Fennoscandian tundra, *Empetrum nigrum* ssp. *hermaphroditum* heaths dominate the windswept heaths while communities rich in *Vaccinium myrtillus* L. occur as strands between *Empetrum* heaths and grass-dominating snow-beds (Oksanen and Virtanen, 1995). Under the greater snow accumulation, the shrubs are higher and species such as *Betula nana* L. and *Salix* spp. are intermixed with *V. myrtillus*. Both tundra heath types are characterized by a continuous bryophyte and lichen cover. To date, little is known about how WS and SA habitats differ in microbial community composition and seasonal trends, and the consequences of these changes in community composition on carbon cycling. Soil microbial communities under a thick snow layer with soil temperatures around 0 ºC have stable conditions that likely enable active soil organic matter (SOM) degradation throughout the winter (Schimel et al. 2004), whereas windswept habitats can experience very low temperatures during winter (Niittynen et al. 2020), leading to a need for the community to adjust to such cold conditions. Microbial communities could thus be expected to be highly divergent between windswept and snow-accumulating tundra habitats.

In this study, we utilized tundra heaths with long-term natural differences in winter-time snow accumulation. The effect of contrasting snow accumulation and subsequent differences in winter soil temperatures on microbial biomass as well as bacterial and fungal community structure were assessed during different seasons. There are indications that the bacterial communities during the

150 growing season are relatively similar in soils of both habitat types and are dominated by stress-
151 tolerant, oligotrophic bacterial taxa such as the Acidobacteriota (Männistö et al. 2013). However,
152 earlier studies of the same tundra sites indicated strong shifts in the relative abundance of
153 dominant bacterial phylotypes in WS heaths especially during spring thaw suggesting that lower
154 winter temperatures and more frequent freeze-thaw cycles may have strong control over the
155 microbial biomass and community structure with a stronger effect in the windswept than in deep
156 snow habitats (Männistö et al. 2013). In this study, we evaluated bacterial and fungal biomass
157 using phospholipid fatty acid (PLFA) and qPCR analyses and characterized the community
158 structures by rRNA gene and ITS amplicon sequencing of soil sampled in mid-winter, early and
159 late growing seasons. The aim was to identify key taxa of the bacterial and fungal communities
160 linked to differences in winter snow accumulation. We hypothesized that (1) differences in the
161 snow accumulation with strong differences in winter soil temperatures lead to divergent patterns in
162 bacterial and fungal biomass between WS and SA tundra heaths during the mid-winter and early
163 growing seasons. We predicted that the more severe freezing and frequent freeze-thaw cycles in
164 WS tundra heaths are associated with lower microbial abundance due to lower microbial activity,
165 and higher turnover, whereas SA tundra heath harbor more stable microbial communities across
166 seasons. We further hypothesized that (2) differences in the winter conditions are associated with
167 differences in the bacterial and fungal community structure, showing a distinct cryotolerant
168 microbial community structure under WS tundra heaths during winter, with only weak differences
169 in the bacterial and fungal communities between the summer and the winter under SA heaths.
170

171 **Materials and Methods**

172 **Field site**

173 The study site was located in the north side of Mt Pikku-Malla fjeld in Malla Nature reserve,
174 Kilpisjärvi, north-western Finland (69°03' 50"N, 20°44'40"E). The mean annual precipitation is 420

175 mm and the mean annual temperature is -1.9°C (Aalto et al. 2018). The bedrock at the sampling
176 sites of this study was formed from siliceous rock materials resulting in acidic barren soil where
177 heaths dominated by the dwarf shrub *Empetrum nigrum* spp. *hermaphroditum* (Hagerup) Böcher
178 prevail (Eskelinen et al. 2009). The tundra heaths are exposed to heavy winds which together with
179 the differences in topography dramatically influence snow accumulation. Areas with high snow
180 accumulation (up to ≥ 1m) are located in depressions and areas sheltered from the winds, while
181 windswept areas remain essentially snow-free throughout the winter (Fig. S1). Soil temperature
182 under thick snow cover is more stable, remaining close to 0°C throughout the winter, while in the
183 windswept heaths, the temperature follows air temperature and may drop down to -15 °C
184 (Männistö et al. 2013; Fig 1). In addition to soil temperature and snow accumulation, variations in
185 topography result in alternating patterns in vegetation. *Empetrum nigrum* dominated especially in
186 the WS heaths while *Vaccinium myrtillus* was more abundant in the SA heaths. *Vaccinium vitis-*
187 *idea* and *Vaccinium uliginosum* were common in both habitat types. Under the higher snow
188 accumulation, the shrub height was higher and species such *Betula nana* L. and *Salix* spp. were
189 abundant. Both tundra heath types were characterized by a continuous bryophyte and lichen
190 cover.

191

192 **Soil sampling**

193 Four plots (2 × 2 m) representing windswept slopes (*i.e.*, dominated by *E. hermaphroditum*) and
194 four plots corresponding to snow-accumulating biotopes (*i.e.*, dominated by *V. myrtillus*) were
195 selected and marked based on earlier snow cover estimates (Männistö et al. 2013) and the type of
196 vegetation. All plots were within 300 m from each other and at least 25 m apart. Soil temperature
197 was recorded once every hour using Hobo U10 temperature loggers (Onset Computer, Bourne,
198 Massachusetts) that were buried 3-5 cm below the soil surface. The soil was sampled from
199 windswept and snow-accumulating tundra heaths in February, June and September 2013 from the

top 5 cm (humus layer) using a soil corer (diameter ca. 2 cm). Composite soil samples of 5 soil cores were taken from each plot. In June and September, the samples were sieved in the field using a 2 mm mesh and immediately frozen in a liquid nitrogen dry shipper. February samples were transported frozen to the lab and sieved after brief thawing. Three sub-samples (0.3 g) were taken from each composite sample and stored at -80 °C until thawed for DNA/RNA extraction.

Soil physico-chemical analyses

The dry matter content of the soil was determined by drying the samples (105 ºC, 12 h) and organic matter (OM) content was analyzed by loss on ignition (475 ºC, 4 h). Soil pH was measured in 1:5 (vol:vol) soil:water suspensions (Denver Instrument Model 220). A sub-sample of ~ 3 g fresh soil was extracted for 2 h with 50 mL of 0.5 M K_2SO_4. Dissolved organic carbon (DOC) concentrations in these extracts were analyzed with a TOC-VCPH/N Total Organic Carbon Analyzer (Shimadzu Corporation, Kyoto, Japan). Total nitrogen, NH_4-N and NO_3-N concentrations were analyzed via flow injection analysis (Quickchem 8000 FIA Analyzer, A83200, Zellweger Analytics, USA). Extractable organic nitrogen (N) was calculated by subtracting inorganic N concentrations from the total. Microbial C and N were extracted from the samples using 0.5 M K_2SO_4 after chloroform fumigation for 18 hours (Brookes et al. 1985), and then analyzed as total extractable N and DOC. Phosphorus was analyzed colorimetrically (Murphy and Riley 1962).

Nucleic acid extraction and cDNA synthesis

Total genomic DNA and RNA were extracted from approximately 0.25 g of soil with slight modifications as described earlier (Männistö *et al.* 2016) using a CTAB-based method by Griffiths *et al*. (2000). Three replicate extractions were processed from each of the 8 plots. Hexadecyltrimethylammoniumbromide (CTAB; 650 μl) extraction buffer and phenol-chloroform-

isoamyl alcohol (25:24:1; pH 8.0; 650 μl) were added together with a mixture of beads to the sample tubes followed by bead beating on a Precellys 24 Dual homogenizer (Bertin Technologies, Montigny-le-Bretonneux, France) for 30 s at 5500 rpm. The bead mixture contained 0.1 mm glass beads (0.3 g), 1.0 mm ceramic beads (0.7 g) and two large (3.5 mm) glass beads (Bio Spec Products Inc., Bartlesville, OK, USA). Samples were further processed as described in Männistö et al. (2016). DNA samples were treated with RNAse A (Thermo Scientific, Waltham, MA, USA) and RNA samples with DNAse I (Thermo Scientific) and converted to cDNA using the Revert Aid H Minus First Strand cDNA Synthesis kit (Thermo Scientific). All solutions used for RNA extraction were treated with 0.1% diethylpyrocarbonate (DEPC). RNA and DNA concentrations were measured using a Qubit fluorometer and Quant-iT RNA and dsDNA HS assay kits (Thermo Scientific), respectively.

Microbial phospholipid fatty acid (PLFA) analyses and quantitative PCR (qPCR)

PLFA and qPCR analyses were used to estimate bacterial and fungal biomass in the tundra soil. Microbial lipids were extracted from ca. 1 g (wet weight) of freeze-dried soil as described previously (Männistö et al. 2016). The phospholipid fatty acid (PLFA) 18:2ω6c was used to indicate fungal biomass [including saprotrophic, ectomycorrhizal and ericoid mycorrhizal fungi (Olsson, 1999; Ruess et al. 2002)], while the sum of PLFAs i15:0, a15:0, 15:0, i16:0, 16:1ω9c, i17:0, a17:0, 17:0, cyclo-17:0, 18:1ω7c and cyclo-19:0 was used to indicate bacterial biomass (Frostegård and Bååth, 1996).

qPCR was performed using the Bio-Rad CFX96 Real-time thermal cycler (Bio-Rad) and SsoAdvanced Universal SYBR Green Supermix (Bio-Rad). 16S rRNA gene copy numbers were quantified using the primer pair Eub341F (CCTACGGGAGGCAGCAG) and Eub534R (ATTACCGCGGCTGCTGG) (Muyzer et al. 1993), and fungal ITS2 region copies with the primer

pair fITS7 (GTGARTCATCGAATCTTTG) (Ihrmark et al. 2012) and ITS4 (TCCTCCGCTTATTGATATGC) (White et al. 1990). All qPCRs were run in technical triplicates of 20 µL and contained 10 µL Supermix, 0.5 µL of each primer (10mM), 7 µL ddH2O and 2 µl template in a 100-fold dilution. PCR conditions for bacterial analysis were 98°C for 2 min followed by 40 cycles of 98°C (5s), 56°C (20s), and for fungal analysis 98°C for 3 min followed by 40 cycles of 98°C (15 s), 61°C (60 s), (following a plate read). Genomic DNA from *Granulicella mallensis* MP5ACTX8 isolate was used as a bacterial and *Laccaria laccata* isolate as a fungal standard.

PCR and Ion Torrent sequencing

First amplification of the V1-V3 region of the 16S rRNA gene was done in duplicates for each DNA/cDNA sample in 20 µl reactions containing 1 µl of 1:50 diluted DNA template, DreamTaq DNA Polymerase (Thermo Scientific), 0.3 µM of each primer (27F 5'-AGAGAGTTTGATCMTGGCTCAG-3', Lane 1991 and 518R 5'-ATTACCGCGGCTGCTGG-3', Muyzer et al. 1993), 3.2 µgof bovine serum albumin and 0.2 mM of dNTP mix. In the second amplification step, primer IonA_bc_27F included adapter IonA (5'-CCATCTCATCCCTGCGTGTCTCCGAC-3') and unique 10-12 bp long barcode sequences before the primer 27F and primer P1_518r included P1 5'-CCTCTCTATGGGCAGTCGGTGAT-3' before the primer 518r to allow Ion Torrent sequencing and assignment to specific samples. The cycling regime for the first PCR included denaturation of 95 °C for 5 min, followed by 25 cycles of 94 °C 30 sec, 55 °C 30 sec and 72 °C 1 min, and a final elongation step of 72 °C for 10 min. The second PCR reaction contained 1 µl of the reaction product of first amplification, and only 15 cycles were run. PCR products were cleaned using the Agencourt AMPure XP magnetic beads purification system (Beckman Coulter, Brea, CA, USA) and quantified with Qubit dsDNA HS Assay Kit (Thermo Scientific). Amplicons were then combined in equimolar concentrations for sequencing. The pooled 16S rRNA gene amplicon libraries were sequenced using Ion Torrent Personal

Genome Machine (Thermo Scientific) at the University of Jyväskylä, Finland. One set of samples (DNA samples of February) was sequenced in 2014 using a 316 v2 chip and all other samples in 2015 using a 314 v2 chip. The sequencing chemistry and Ion Torrent software was updated multiple times between these two runs, potentially affecting the results, and therefore the bacterial DNA sequences from February were not compared with the other sampling seasons (see Statistical Analyses). Amplification of the ITS2 region of fungal rRNA operons was performed as a 2-step procedure recommended by Berry et al. (2011). The first amplification step was done in triplicate for each sample (1 µl of 1:50 dilution) in a 10 µl reaction and the second step in a single 50 µl reaction for each sample (1µl of PCR product from step 1), both amplification steps using Phusion High-Fidelity DNA Polymerase (Thermo Scientific), Phusion HF Buffer and 0.2 mM of dNTPs and each primer (ITS7 5'-GTGARTCATCGAATCTTTG-3', Ihrmark et al. 2012 and ITS4 5'-TCCTCCGCTTATTGATATGC-3', White et al. 1990). In the second amplification step, ITS7 primer included the adapter P1 5'-CCTCTCTATGGGCAGTCGGTGAT-3' and ITS4 primer included the adapter IonA 5'-CCATCTCATCCCTGCGTGTCTCCGACTCAG-3' and unique 10 bp long barcode sequences at the beginning of the primer to allow Ion Torrent sequencing and assignment to specific samples. The cycling regime for the first step was: initial denaturation of 98 °C for 1 min, followed by 25 cycles of 98 °C 10 sec, 54 °C 20 sec and 72 °C 30 sec, and a final elongation step of 72 °C for 7 min. For the second step cycling regime was the same as in the first except for changing the cycle number to 10 and the annealing temperature to 57 °C. Fungal ITS amplicons were sequenced at Biocenter Oulu Sequencing Center (Univ. Oulu, Oulu, Finland). PCR products were first cleaned using the Agencourt AMPure XP magnetic beads purification system and BioMek4000 Laboratory Automation Workstation (Beckman Coulter) followed by purity checking and quantification using MultiNA (MultiNA Microchip Electrophoresis System and DNA-1000 kit; Shimadzu, Kyoto, Japan) and PicoGreen (Thermo Scientific) according to manufacturers' instructions. Amplicons were then combined in equimolar concentrations for Ion Torrent PGM sequencing with 314 v2 chip.

299

300 **Bioinformatics**

301 Bacterial sequence reads from the two sequencing efforts (total 3,005,260 and 2,666,670 reads)
302 were demultiplexed, quality filtered and merged with the following adjustments using QIIME 1.9.1
303 (Caporaso et al. 2010): minimum length of 300 bp, maximum of 1 mismatch in primer sequences,
304 and minimum mean quality score of 25 within 50 bp window size. We employed a reference-based
305 operational taxonomic unit (OTU) picking against SILVA release 128 99% identity reference
306 database (Quast et al. 2013), removing chimeras, and clustering all sequences using USEARCH
307 6.1 (Edgar 2010; Edgar et al. 2011) with a sequence similarity value of 97%. Taxonomy was
308 assigned for representative sequences using a naïve Bayesian RDP classifier (Wang et al. 2007)
309 against SILVA 99% identity majority taxonomy strings with a confidence threshold of 50%.
310 Representative sequences from each OTU were aligned to the SILVA 99% identity reference
311 alignment using PyNAST (Caporaso et al. 2009) and a phylogenetic tree was built using FastTree
312 (Price et al. 2009). After removing singletons (OTUs represented by a single sequence) and
313 alignment failures from the data, 1,249,249 reads were obtained from all samples with an average
314 of 10,498 reads per sample (min 3314 and max 32,820). For downstream analyses, all samples
315 were rarefied by random sampling (without replacement) to an equal sequence number of 3300 to
316 minimize bias due to different sequencing efforts across samples.

317 ITS sequence reads (total 701,430 reads) were demultiplexed and quality filtered with the
318 following adjustments using QIIME 1.9.1 (Caporaso et al. 2010): minimum length of 200 bp, the
319 maximum length of 600 bp, maximum of 1 mismatch in primer sequences, and minimum mean
320 quality score of 20 within 50 bp window size. We employed a chimera check using UCHIME
321 (Edgar et al. 2011) and sequences were then clustered into operational taxonomic units (OTUs)
322 using UCLUST (Edgar 2010) with a sequence similarity value of 97%. Taxonomy was assigned for
323 representative sequences using BLAST (Altschul et al. 1990) against UNITE v.7.1 97% threshold

reference database (Kõljalg et al. 2013) with 90% identity. After removing singletons (OTUs represented by a single sequence) and non-fungal hits from the data, 404,561 reads were obtained from all samples with an average of 6321 reads per sample (min 1486 and max 10,579). For downstream analyses, all samples were rarefied by random sampling (without replacement) to an equal sequence number of 1400 to minimize bias due to different sequencing effort across samples.

Raw sequence data and associated metadata were deposited in GenBank with the Bioproject accession no. PRJNA1080106.

Statistical analyses

Differences in bacterial and fungal community structure were analyzed using permutational analysis of variance (PERMANOVA, Anderson, 2001) and visualized with principal coordinate ordination (PCO). For the PERMANOVA and PCO analyses, bacterial and fungal OTU data were Hellinger-transformed and Bray-Curtis dissimilarity matrices used as the resemblance matrices. Habitat (windswept, WS or snow-accumulating, SA) and sampling season (winter, early or late growing season) were used as fixed factors and plot as a random factor nested in habitat. When significant interactions were detected for habitat and season, pairwise PERMANOVA was performed on the respective terms. All PERMANOVA analyses were performed with 999 random permutations PERMANOVA and ordination analyses were performed using the PERMANOVA+ add-on (Anderson et al. 2008) for PRIMER v7 (Clarke and Gorley 2015). Data analysis indicated that bacterial communities of winter DNA samples deviated strongly from all other samples (derived from DNA or RNA) as illustrated by a PCO ordination (Fig. S2). This deviation may be, at least partially, due to a sequencing bias as the winter DNA -derived bacterial

communities were sequenced earlier than the other samples. Samples of the different sequencing runs were sequenced using a different chip and sequencing chemistry and the also the server software was updated between the runs. Therefore, to avoid potential sequencing bias the February DNA data were not compared with other sampling points or with RNA-derived community structure in the statistical analysis.

The effect of habitat, sampling season and their interaction on microbial biomass proxies (16S rRNA gene and ITS copies, total PLFAs, bacterial PLFAs, fungal PLFA, bacterial/fungal PLFA ratio) and soil physico-chemical properties as well as on the abundance of ten most abundant bacterial and fungal genera were tested using linear mixed effect model (LME) with habitat and season as fixed factor and plot as random factor. Sampling season was assigned as repeated factor with site as a subject and AR1 as the covariance structure. When significant interactions were detected for habitat and season, habitats were further tested separately with a Least Significant Difference test as a post hoc –test under the linear mixed model. Logarithmic transformations were used as necessary to meet the assumptions the linear mixed model. LME tests for microbial biomass and soil parameters were conducted using IBM SPSS 29.0 software. Distance based linear modelling (DistLM) (Legendre and Anderson 1999; Anderson et al. 2008) was used to determine the extent to which soil variables explain bacterial and fungal community structure in WS and SA tundra heaths. Multicollinearity between variables was first tested using the Draftsman Plot function and spearman correlations in PRIMER v7 (Clarke and Gorley 2015) and from variables that correlated by more than 0.9, only one was picked. Of the nitrogen forms, total and organic N correlated by 0.96 and N_{org} was therefore omitted from the analysis. Logaritmic transformations were used for the same variables as for the LME tests (N_{tot}, NH_4, P_{tot} and P_{mic}). Marginal tests identified the influence of individual soil variables on bacterial (DNA and RNA) and fungal community structure without considering the effect of other variables. To identify the soil parameters that in combination explained bacterial and fungal community structure, DistLM model was utilized with stepwise selection procedure and corrected Akaike information criterion (AICc) as

the selection criteria with 999 permutations. The resulting models were visualized using distance based redundancy analysis (dbRDA) plots. DistLM analyses and dbRDA plots were done performed using the PERMANOVA+ add-on (Anderson et al. 2008) for PRIMER v7 (Clarke and Gorley 2015).

Results

Soil physico-chemical properties and microbial biomass in windswept and snow-accumulating tundra heaths

Soil temperature differed strongly in windswept (WS) vs. snow-accumulating (SA) tundra (Fig. 1). The average soil temperature from September 2012-September 2013 was 0.1°C in the WS plots and 2.4°C in SA plots. During the coldest months (December-March), the average soil temperature was -7.1°C and -1.0°C in the WS and SA plots, respectively. On the other hand, due to earlier spring thaw and less insulating vegetation cover, the WS plots were warmer in June with an average soil temperature of 8.4 °C compared to 7.0°C in the SA plots.

Linear mixed effect model indicated that there were no significant differences in soil pH, moisture or OM content between WS and SA heaths, but they differed in nutrient availability. Total nitrogen (Ntot, $F=21.34$, $p=0.004$) , organic nitrogen (Norg, $F=17.053$, $p=0.007$), NH_4-N ($F=7.534$, $p=0.034$) and total phosphorus (Ptot, $F=10.675$, $p=0.017$) availability were significantly higher in the SA than WS heaths throughout the sampling year. On the other hand, N stored in microbial biomass (Nmic, $F=5.353$, $p=0.060$) tended to be higher in the WS than under SA heaths. Sampling season had a significant impact on soil N availability, the concentrations of all N forms were at their lowest in samples collected in late growing season (Table 1 and Supplementary Table S1). However, when the habitats were tested separately, sampling season had a significant effect on N_{tot} only in the WS heaths ($p=0.012$ between winter and early growing season and $p<0.001$ between other

399 sampling seasons), while NO_3 availability was significantly different between winter and early
400 growing season (p=0.008) and early and late growing season (p=0.001) in WS heaths, and winter
401 and early growing season (p=0.049) and winter and late growing season (p=0.003) in SA heaths.
402
403 Microbial biomass was estimated using soil PLFA analysis and qPCR of bacterial 16S rRNA gene
404 and fungal ITS region copy numbers (Figs. 2 and 3). The Linear mixed effect model indicated that
405 there were no significant differences in the abundance of total PLFAs between the different tundra
406 heaths or sampling dates. Bacterial PLFAs were higher in the SA than WS plots and these
407 decreased towards the late growing season, but the differences were not statistically significant.
408 The fungal PLFA marker was in higher abundance in the WS heaths (F=16.208, p=0.007) and
409 tended to be lower (F=2.732, p=0.086) in the early and late growing season samples. The fungal
410 to bacterial PLFA ratio was higher in WS heaths (F=82.804, p<0.001) and was lowest during June
411 (F=4.728, p=0.019) (Fig. 2; Supplementary Table S1).
412
413 Bacterial 16S rRNA gene copy numbers were significantly different (F=31.165, p=0.001;) between
414 WS and SA heaths as well as at different sampling seasons (F=38.792, p<0.001) and there was a
415 significant habitat × season interaction (F=54.388, p<0.001; Table S1).This was attributed to the
416 significantly lower copy numbers in the WS plots during late growing season (p<0.001). LME test
417 indicated no significant main effect of habitat on fungal copy numbers, but when the habitats were
418 tested separately, pairwise tests indicated that in WS heaths, ITS copy numbers were significantly
419 lower p<0.001) in late growing season than in winter or early growing season (Fig. 3; Table S1).
420
421 **Bacterial community structure in windswept and snow-accumulating tundra heaths**
422 Bacterial community composition was characterized by 16S rRNA gene (representing total
423 community) and reverse transcribed 16S rRNA (representing active community) amplicons. Due to

424 a potential bias associated with the differences in sequencing (see Materials and Methods), winter
425 bacterial DNA samples were excluded from the multivariate statistics (PCO, PERMANOVA) and
426 not compared to data of the other seasons.
427
428 PCO ordination indicated the greatest differences between the DNA (total) and RNA (active)
429 derived bacterial community structures (Fig. S3) which separated the samples into two main
430 groups along the first axis that explained most of the variance. To delineate the effects of habitat
431 and sampling season on the total vs. active communities, the DNA and RNA-derived datasets
432 were analyzed separately. PCO ordination grouped both total and active communities from WS
433 and SA tundra heaths separately (Fig. 4). This was supported by PERMANOVA analysis in which
434 habitat explained slightly more of the community variation than sampling season (Table 2).
435 Pairwise PERMANOVA analysis for the WS and SA habitats separately indicated that the active
436 bacterial communities were significantly different in all sampling seasons (p=0.001-0.004) except
437 in SA heaths between early and late growing season. Total bacterial communities were different in
438 WS heaths (p=0.001) but not in SA heaths (p=0.265) between early and late growing season.
439
440 Both tundra heath types were dominated by Actinomycetota, Pseudomonadota (mainly class
441 Alphaproteobacteria) and Acidobacteriota (Fig.5). At the genus level, the most dominant
442 Actinomycetota were *Acidothermus* spp., *Mycobacterium* spp. and unknown taxa of the class
443 Acidimicrobiales. The most abundant Acidobacteriota were *Granulicella* spp., *Bryobacte*r spp.,
444 *Edaphobacter* spp., unknown Acidobacteriia (subdivision (SD) 1) and unknown SD 2
445 Acidobacteriota. The most abundant Pseudomonadota were unknown members of the
446 Acetobacteraceae, *Roseiarcus* spp., *Bradyrhizobium* spp., *Variibacter* spp., *Rhodoplanes* spp.,
447 unknown genera of Caulobacteraceae and Xanthobacteraceae and the DA111 group of
448 Alphaproteobacteria. The same genera dominated both in the DNA and RNA amplicons but with
449 differences in the relative abundances (Fig. 5; Supplementary Fig S3). Of the Alphaproteobacteria,

450 unknown genera within the Acetobacteraceae and Xanthobacteraceae were more abundant in the
451 RNA-derived community while *Bradyrhizobium* spp. were more abundant in the DNA. Similarly,
452 *Acidothermus* spp. (Actinomycetota) were significantly more abundant in RNA while
453 *Mycobacterium* spp. were more abundant in the DNA-derived community. Of the Acidobacteriota,
454 unknown members of SD2 and SD1 were more abundant in the DNA- than RNA-derived
455 community.
456
457 Comparison of the active bacterial communities between WS and SA tundra heaths revealed
458 relatively small differences in the dominant bacterial groups (Fig. 5; Supplementary Fig S4). Of the
459 ten most dominating active bacterial genera, unknown genera within the family Acetobacteraceae
460 and members of Acidobacteriota were significantly affected by the habitat (LME, $p<0.05$), but this
461 interacted with the season. Acetobacteraceae were more abundant in WS heaths only in early and
462 late growing season. Of the Acidobacteriota, unknown Acidobacteriaceae were more abundant in
463 the SA tundra heaths in the early and late growing season, *Granulicella* spp. were more abundant
464 in WS tundra heaths but only in the early growing season, while members of SD2 Acidobacteriota
465 were more abundant in SA tundra in the late growing season. The abundance of different genera
466 of Pseudomonadota was generally more affected by sampling season than the habitat (Fig. S4).
467
468 **Fungal communities in windswept and snow-accumulating tundra heaths**
469 PCO and PERMANOVA analyses indicated that fungal communities were structured more by the
470 habitat than by sampling season (Fig. 4, Table 2). Moreover, the communities were more
471 dispersed in the SA than WS heaths. Pairwise PERMANOVA analysis indicated that there were no
472 differences between winter and early growing season community structure in the WS tundra
473 heaths while all other sampling seasons differed in WS and SA heaths ($p=0.001$-0.049). Fungal
474 communities under both tundra heaths were dominated by Basidiomycota, Ascomycota and
475 Mucoromycota. Basidiomycota were the most abundant fungi under both WS and SA heaths and

were especially dominant in the winter samples. Of the Basidiomycota, the order Agaricales dominated in both habitats with *Clavaria* spp. as the most dominant genus in WS heaths and *Cortinarius* spp. more abundant in the SA heaths. Group B Sebacinales were more associated with the WS heaths. Members of the order Helotiales were the dominant Ascomycota both in WS and SA heaths while members of Chaetothyriales were more abundant in the WS heaths (Fig. 6).

Of the ten most abundant genera, *Clavaria* spp., unknown Sebacinales, unknown Chaetothyriales and unknown Ascomycota were significantly (LME; $p<0.05$) more abundant in the WS tundra heaths while *Mortierella* spp. were more abundant in the SA heaths. Members of *Cortinarius* were more abundant in the SA heaths, but due to the high variation between samples, the difference was not significant. *Rhizoscyphus* and other Helotiales were abundant in both heath types and tended to be more abundant in the WS heath, but the difference was not statistically significant (Supplementary Fig S5).

Effect of soil physico-chemical properties on bacterial and fungal community structure

Distance based linear modelling was used to determine the contribution of soil factors on bacterial and fungal community structures. Marginal tests indicated that except for NO_3, all nine tested soil factors had a significant impact on both bacterial and fungal community structure (Supplementary Table S2, Suppl. Fig S6). Total nitrogen explained most of the variation of bacterial and fungal community structure and was also among the variables in the best DistLM model that predicted the community structure. Active, RNA derived bacterial community structure was predicted best by N_{tot}, P_{mic}, OM% and N_{mic}. while total, DNA derived bacterial community (with only early and late growing season samples) was predicted by pH, N_{tot} and N_{mic} and fungal community by Ntot, Nmic, pH and OM% (Suppl. Fig. S6). The models explained 20.6, 20.0 and 26.3% of the variation in RNA derived, DNA derived bacterial and fungal community structure, respectively.

Discussion

Windswept and snow-accumulating tundra heaths are characterized by large differences in soil temperature. In addition to strong differences in the winter soil temperatures, there is a difference in the amplitude of annual temperature variation. Due to earlier snowmelt and lower insulation from vegetation, the windswept heaths are associated with high-temperature fluctuation and, depending on the air temperatures, also prone to frequent freeze-thaw cycles during spring (Männistö et al. 2013; this study). These differences in topography lead to a spatially heterogeneous snow cover depth and soil temperatures that in turn form predictable patterns in the dominant vegetation (Oksanen and Virtanen 1995, Niittynen et al. 2020), but so far, how these differences drive microbial community composition has remained uninvestigated. Supporting our hypothesis that the topographic differences and associated consequences on vegetation, soil temperatures, nutrient availability as well as the quantity and quality of organic matter modify soil microbial community composition, PLFA, qPCR and sequencing of 16S rRNA genes and the ITS region indicated distinct differences in the bacterial and fungal communities in WS vs. SA tundra heaths. Contrasting our hypothesis, however, the seasonal trends were either uniform between the WS and SA tundra heaths or amplified towards the end of the growing season rather than being greatest in winter when the difference in soil temperatures was the greatest. These results imply that differences in the bacterial and fungal communities in WS and SA tundra heaths across different seasons were likely driven by vegetation, soil nutrients and carbon substrates rather than by soil temperature *per se*.

PLFA and qPCR analyses indicated generally higher fungal abundance in the WS tundra heaths while bacterial PLFAs tended to be higher in the SA tundra heaths with higher nutrient availability. This is in line with other studies from tundra showing positive correlations of bacterial abundance with nutrient availability (Eskelinen et al. 2009; Stark et al. 2012). Contrary to our hypothesis, there

were only minor differences in the bacterial and fungal gene copy numbers between WS and SA heaths in winter, but differences were magnified toward the end of the growing season when both bacterial and fungal gene copy numbers dropped in the WS heaths, coinciding with drastically lower soil N and P concentrations. The parallel trends in bacterial and fungal gene copy numbers and nutrient availability indicate that limitations in soil nutrient availability may have contributed to increased microbial turnover during the growing season in WS heaths, which supports earlier findings of strong competition for nutrients between plants and microbes in Arctic nutrient-poor soils (Jonasson et al. 1996; Stark and Kytöviita, 2006; Stark et al. 2023). Owing to a strong nutrient limitation, tundra soil carbon and nitrogen cycles are strongly coupled, and microbial N immobilization and even soil microbial biomass may be regulated by plant nitrogen uptake (Jonasson et al. 1999; 2001, Schimel and Bennett 2004). Following the patterns of plant nitrogen uptake, soil nitrogen availability often decreases during the growing season, leading the soil microbial communities to become increasingly N-limited towards the end of the growing season (Stark and Kytöviita 2006; Weintraub and Schimel 2005a; 2005b; Wallenstein et al. 2009). This induces a strong seasonality of microbial biomass and activities that may be at their highest in early spring and late autumn when the plant activity is at its lowest (Stark and Kytöviita 2006; Stark and Väisänen 2014). The decrease of bacterial and fungal gene copy numbers towards the end of the growing season in the nutrient-poor windswept tundra heaths is thus in line with microbial communities being driven more by nutrient limitations than directly by the winter temperatures.

Another factor that may have contributed to the decline in microbial biomass in WS tundra heaths towards the end of the growing season could be decreased availability of labile C that would increase turnover of microbial biomass. In contrast, some studies suggest that increased winter-time decomposition under increased snow depth may decrease microbial respiration in the following growing season due to reduced availability of labile C substrates (Semenchuk et al. 2016; Sullivan et al. 2020). Differences in vegetation between WS and SA sites, however, likely cause differences in soil C and N by multiple mechanisms. *Empetrum nigrum* that was especially

552 dominant in the WS sites produce allelophatic compounds and slowly decomposable litter that
553 generally decelerate soil nutrient and carbon cycles (Bråthen et al. 2010; Vowles and Björk 2018).
554 Moreover, the known and putative ErM fungi, which were more dominant is the WS sites, produce
555 recalcitrant necromass that further increases the stability of the organic matter and reduces the
556 availability of labile C and N forms (Clemmensen et al. 2015; 2021). Snow-cover related to
557 topography may thus be an important microclimatic driver of both microbial community
558 composition and SOM dynamics.

559 The higher fungal PLFA abundance and fungal-to-bacterial ratio in the windswept tundra heaths
560 (Table S1) was associated with clear differences between the fungal communities in WS and SA
561 tundra heaths. While known ericoid mycorrhizal fungi, such as *Rhizoscyphus* spp. and other
562 *Helotiales* (Clemmensen et al. 2015; Leopold et al. 2016) were abundant in both, WS and SA
563 tundra heaths (Fig. 6), ectomycorrhizal fungi, especially the genus *Cortinarius*, were more
564 abundant in some sites of the SA tundra heaths corresponding to higher abundance of
565 ectomycorrhizal dwarf shrubs (*Betula nana* and *Salix* spp.) under SA heaths. The low abundance
566 of *Cortinarius* spp. in WS heaths may, however, also be explained by the sensitivity of these fungi
567 to freezing (Ma et al. 2001) as some *Cortinarius* species have been shown to benefit from
568 increased snow depth in dry tundra sites of Alaska (Morgado et al. 2016). Members of the genus
569 *Clavaria* were the most abundant fungal taxa at the genus level and significantly more abundant in
570 the WS tundra heaths. The most abundant OTU of the whole fungal data set (>11% of all
571 sequence reads) was related to *Clavaria* sequences from Arctic soils (Dahl et al. 2017; Deslippe et
572 al. 2012) and *Clavaria argillacea* sampled from Greenland, indicating an association to Arctic
573 ecosystems. *Clavaria* has been reported as the dominant taxa in tundra soils of Alaska
574 (Semenova et al. 2016), Greenland (Voříšková et al. 2019) and in Raisduoddar fell in northern
575 Norway located close to our study site (Ahonen et al. 2021). *Clavaria* spp. are considered
576 saprotrophic, but they have been found abundantly in hair roots of ericoid shrubs such as
577 *Vaccinium uliginosum* (Yang et al. 2018), *Vaccinium corymbosum* (Li et al. 2020) and bidirectional

578 nutrient transport between a *Clavaria* and ericaceous plant species have been reported
579 (Englander and Hull., 1980), indicating that they may have symbiotic associations with the ericoid
580 shrub vegetation in nutrient-poor tundra heaths. *Clavaria* was identified as one of the most
581 dominant taxa associated with roots of the Ericaceae shrub *Cassiope tetragona* growing in
582 Svalbard (Lorberay et al. 2017), further suggesting its importance in Ericaceae shrub-dominated
583 tundra heaths. The higher abundance in the more nutrient-poor WS tundra heaths in this study
584 suggests a role of *Clavaria* spp. in nutrient accessibility and transport between/for the ericoid
585 vegetation. Furthermore, members of *Clavaria* and Clavariaceae have been associated with
586 freeze-thaw tolerant fungal communities in soil from Northern Sweden (Perez-Mon et al. 2020),
587 suggesting their resistance to more extreme winter conditions which may contribute to their
588 abundance in the WS heaths.

589 Other fungal taxa that were consistently more abundant in the WS tundra heaths were members of
590 the order Chaetothyriales and the family Serendipitaceae of the order Sebacinales (group B).
591 Sebacinales comprises a diverse group of cryptic organisms that are considered to form symbiotic
592 relationships with many types of vegetation (Weiß et al. 2016; Leopold et al. 2016), including
593 ericoid mycorrhizal associations with Ericaceae shrubs (Selosse et al. 2007; Vohník et al. 2016).
594 Similar to *Clavaria*, Sebacinales was reported as the dominant order of the roots of *Cassiope*
595 *tetragona* and *Bistorta vivipara* in Svalbard where they were suggested to play an important role in
596 the Arctic tundra ecotone either as mycorrhizae or as endophytes (Blaalid et al. 2014; Lorberau et
597 al. 2019). However, the ecological role of the Sebacinales in these ecosystems require further
598 research as OTUs both in this study and those from Svalbard had low sequence similarities to
599 known Sebacinales, a taxonomically and functionally a diverse group with many unknown
600 representatives (Oberwinkler et al. 2013)

601 PERMANOVA analysis indicated significant differences in the bacterial communities between WS
602 and SA tundra heaths during all sampling seasons but contrary to our hypothesis there were

603 relatively minor differences in the dominant bacterial taxa during winter. Bacterial communities
604 were dominated by members of Actinomycetota, Pseudomonadota (Alphaproteobacteria) and
605 Acidobacteriota. These groups have been shown to dominate the soil and mycosphere of ericoid
606 shrubs (Timonen et al. 2016), indicating their link to the shrub vegetation and/or associated fungi.
607 Actinomycetota, Pseudomonadota and Acidobacteriota were reported as the dominant taxa also in
608 metagenomes and metatranscriptomes of tundra soil sampled from the same area (Pessi et al.
609 2022; Viitamäki et al. 2022). Our earlier studies of the same tundra habitats indicated a high
610 dominance of Acidobacteriota in clone libraries of both WS and SA tundra heaths (Männistö et al.
611 2013). In this study, the dominance of Acidobacteriota was lesser with a greater abundance of
612 Actinomycetota-associated reads. This increase in the share of Actinomycetota is likely due to
613 differences in the DNA and RNA extraction protocol with stronger beat beating conditions used in
614 our current protocol (described in Männistö et al. 2016). The most abundant bacterial OTUs were
615 associated with the Actinomycetota genus *Acidothermus* which comprised ca. 20 % of all reads
616 and was especially dominant in the RNA-derived bacterial community both in WS and SA tundra
617 heaths. *Acidothermus* spp. was recently reported as one of the most dominant genus-level taxa
618 also in metagenomes and transcriptomes of soils sampled from the same area (Viitamäki et al.
619 2022). They were especially abundant in acidic shrub-dominated heaths, indicating that this taxon
620 may have an important role in the organic-rich, nutrient-poor tundra soils. Members of
621 Acidothermaceae were abundant also in alpine soils, where they increased with expansion of
622 ericaceous shrubs (Broadbent et al. 2022) further indicating their association with ericaceous
623 vegetation. The only described species of this genus is a thermophilic cellulose degrader
624 (Mohagheghi et al. 1986) indicating that the role of tundra soil *Acidothermus* spp. may be
625 associated with the decomposition of the large plant-derived organic stocks. As *Acidothermus* spp.
626 belong to the order Frankiales which contain well-known nitrogen-fixing species (Gtari et al. 2012)
627 that may rise the question of whether the high abundance of these Actinomycetota is connected
628 also to the nitrogen limitations of the habitat.

629 The most abundant class-level taxa in both WS and SA tundra soils were members of
630 Alphaproteobacteria. The abundance and role of many of these alphaproteobacterial taxa may be
631 associated with nitrogen acquisition as they are associated with known nitrogen-fixing genera
632 (Tsoy et al. 2016). *Bradyrhizobium* and other Alphaproteobacteria were found to be dominant
633 members of the denitrifier populations in the tundra soils of Kilpisjärvi where they were reported to
634 encode terminal oxidases that are active both under highly aerobic conditions and those with high
635 oxygen affinity (Pessi et al. 2022). This type of adaptation would give a competitive advantage for
636 growth under waterlogged (spring) and dry conditions. *Bradyrhizobium* and many other
637 alphaproteobacterial taxa have been also reported as dominant lignin-decomposing taxa in
638 Alaskan tundra soils (Tao et al. 2020), indicating that in addition to a putative role in nitrogen
639 cycling their abundance may be explained by their role in the decomposition of recalcitrant organic
640 matter in organic-rich soils. The relatively small differences between bacterial communities in WS
641 and SA tundra heaths may be due to the versatility of the dominant bacterial groups, with putative
642 roles both in decomposition and nutrient acquisition. However, additional studies are needed to
643 understand the mechanisms associated with these communities.

644 Although differences in vegetation and its mycorrhizal associations were likely important
645 determinants for the soil microbial community composition, soil physico-chemical properties
646 contributed significantly to both the bacterial and fungal community structure. Based on the DistLM
647 model, the analyzed soil variables (pH, OM, different N and P forms) explained roughly 20% and
648 26% of the variation in bacterial and fungal community structures, respectively. Apart from nutrient
649 availability, pH and soil organic matter were key determinants of active bacterial and fungal
650 community structure. Of the analyzed soil properties, particularly soil pH has been shown to
651 control the bacterial community structure in the same area (Männistö et al. 2007) as well as
652 bacterial and fungal community structure globally (Lauber et al. 2009; Teresoo et al 2014).
653 Although there were no significant differences is soil pH between the WS and SA sites, and the
654 variation among different sample replicates was small, soil pH contributed significantly to the

655 variation of bacterial and fungal community structures also in this study. However, as the soil pH
656 was below 5 in all sites, the bacterial and fungal communities were dominated by acid-tolerant and
657 oligotrophic taxa, which may constitute an important factor behind the similarities of the
658 communities between WS and SA tundra heaths.

659 **Conclusions**

660 As hypothesized, we found clear differences in the soil microbial communities between windswept
661 and snow-accumulating tundra heaths. Snow-cover related to topography may thus be an
662 important microclimatic driver of both microbial community composition and soil C and N
663 dynamics. Windswept heaths experienced very low wintertime soil temperatures and strong
664 seasonal fluctuations, which drastically differed from the more stable soil temperature regimes of
665 the snow-accumulating heaths, but contrary to prediction, the soil microbial communities differed
666 the most during the late growing season rather than during winter. Further contrasting predictions,
667 we did not detect distinct cryotolerant communities in WS heaths during winter. A higher
668 abundance of fungal PLFAs and a lower nutrient availability in the WS heaths together with the
669 differing fungal community composition between the WS and SA heaths suggested that these
670 communities were represented by stress-tolerant organisms adapted to nutrient-poor and cold
671 soils. Previous studies have indicated that these types of microbial communities may be rather
672 insensitive to extreme temperatures (Männistö et al. 2018). Instead, the seasonal patterns in
673 microbial biomass and community composition closely followed the seasonal patterns in soil
674 nutrient availability, especially in the more nutrient-limited WS tundra heaths. These results
675 suggest that, rather than directly through low wintertime soil temperatures, topographic differences
676 shape soil microbial communities through modifying the dominant vegetation and soil nutrient
677 availability. This could partially explain why different snow-manipulation experiments have found
678 inconsistent effects of snowpack on microbial community structure and function, ranging from no
679 effect to transient or legacy effects on bacterial and fungal communities in tundra, forest, and
680 alpine soils (Aanderud et al. 2013; Gavazov et al. 2017; Männistö et al. 2018; Morgado et al. 2016;

Mundra et al. 2016; Ricketts et al. 2016; Voříšková et al. 2019). Future experimental studies on Arctic soils should thus include several habitat types with divergent dominant vegetation and nutrient levels to fully separate the direct and indirect effects of temperature.

In the future, the ongoing climate warming will lead to more frequent freeze-thaw cycles and a lower duration and insulation of the snow cover (Bintanja and Andry 2017; McCrystall et al. 2021, Serreze et al. 2021). According to our findings from current topographic gradients in snow accumulation, owing to the high stress-tolerance of soil microbial communities in acidic soils with low temperatures (Männistö et al. 2018), these climatic changes may potentially have a minor role for future soil microbial communities. Instead, shifts in microbial community composition in response to climate warming will likely be largely mediated by shifts in the dominant vegetation and corresponding effects on mycorrhizal associations as well as substrate and nutrient availability for soil microorganisms. Assuming that the ongoing expansion of deciduous shrubs continues across the circumpolar Arctic (e.g., Myers-Smith et al. 2020), counterintuitively, soil microbial communities similar to what we detected for snow-accumulating tundra heaths might therefore increase in coverage.

Acknowledgments

We thank Sirkka-Liisa Aakkonen and Sari Välitalo for their contribution in the sample processing and soil analyses. This study was funded by the Academy of Finland (decision numbers 252323, 310776 and 323063). MMH was funded through the U.S. National Science Foundation (Award Number OCE 2129351).

References

Aalto J, Scherrer D, Lenoir J *et al.* Biogeophysical controls on soil-atmosphere thermal differences: implications on warming Arctic ecosystems. *Environmental Research Letters* 2018;**13**:074003.

Aanderud ZT, Jones SE, Schoolmaster DR *et al.* Sensitivity of soil respiration and microbial communities to altered snowfall. *Soil Biology and Biochemistry* 2013;**57**:217–27.

Ahonen SHK, Ylänne H, Väisänen M *et al.* Reindeer grazing history determines the responses of subarctic soil fungal communities to warming and fertilization. *New Phytologist* 2021;**232**:788–801.

Altschul SF, Gish W, Miller W *et al.* Basic local alignment search tool. *Journal of Molecular Biology* 1990;**215**:403–10.

Anderson MJ. A new method for non-parametric multivariate analysis of variance. *Austral Ecology* 2001;**26**:32–46.

Anderson M.J., Gorley R.N. & Clarke K.R. 2008. PERMANOVA+ for *PRIMER: Guide to Software and Statistical Methods.* PRIMER-E: Plymouth, UK.

Berry D, Mahfoudh KB, Wagner M *et al.* Barcoded Primers Used in Multiplex Amplicon Pyrosequencing Bias Amplification. *Applied and Environmental Microbiology* 2011;**77**:7846–9.

Bintanja R, Andry O. Towards a rain-dominated Arctic. *Nature Climate Change* 2017;**7**:263–7.

Blaalid R, Davey ML, Kauserud H *et al.* Arctic root-associated fungal community composition reflects environmental filtering. *Molecular Ecology* 2014;**23**:649–59.

Bråthen KA, Fodstad CH, Gallet C. Ecosystem disturbance reduces the allelopathic effects of Empetrum hermaphroditum humus on tundra plants. *Journal of Vegetation Science* 2010;**21**:786–95.

Broadbent AAD, Bahn M, Pritchard WJ *et al.* Shrub expansion modulates belowground impacts of changing snow conditions in alpine grasslands. *Ecology Letters* 2022;**25**:52–64.

729 Broadbent AAD, Snell HSK, Michas A *et al.* Climate change alters temporal dynamics of alpine
730 soil microbial functioning and biogeochemical cycling via earlier snowmelt. *ISME J*
731 2021;**15**:2264–75.
732 Brookes PC, Kragt JF, Powlson DS *et al.* Chloroform fumigation and the release of soil nitrogen:
733 The effects of fumigation time and temperature. *Soil Biology and Biochemistry* 1985;**17**:831–5.
734 Buckeridge KM, Grogan P. Deepened snow increases late thaw biogeochemical pulses in mesic
735 low arctic tundra. *Biogeochemistry* 2010;**101**:105–21.
736 Caporaso JG, Bittinger K, Bushman FD *et al.* PyNAST: a flexible tool for aligning sequences to a
737 template alignment. *Bioinformatics* 2009;**26**:266–7.
738 Caporaso JG, Kuczynski J, Stombaugh J *et al.* QIIME allows analysis of high-throughput
739 community sequencing data. *Nature Methods* 2010;**7**:335–6.
740 Clarke, K.R., Gorley, R.N. 2015. *Getting started with PRIMER v7.* PRIMER-E: Plymouth, UK.
741 Clemmensen KE, Durling MB, Michelsen A *et al.* A tipping point in carbon storage when forest
742 expands into tundra is related to mycorrhizal recycling of nitrogen. *Ecology Letters*
743 2021;**24**:1193–204.
744 Clemmensen KE, Finlay RD, Dahlberg A *et al.* Carbon sequestration is related to mycorrhizal
745 fungal community shifts during long-term succession in boreal forests. *New Phytologist*
746 2015;**205**:1525–36.
747 Convey P, Coulson SJ, Worland MR. *et al.* The importance of understanding annual and shorter-
748 term temperature patterns and variation in the surface levels of polar soils for terrestrial
749 biota. *Polar Biol*: 2018 **41:** 1587–1605. https://doi.org/10.1007/s00300-018-2299-0
750 Dahl MB, Priemé A, Brejnrod A *et al.* Warming, shading and a moth outbreak reduce tundra
751 carbon sink strength dramatically by changing plant cover and soil microbial activity. *Scientific*
752 *Reports* 2017;**7**:16035.
753 Deslippe JR, Hartmann M, Simard SW *et al.* Long-term warming alters the composition of Arctic
754 soil microbial communities. *FEMS Microbiology Ecology* 2012;**82**:303–15.

Edgar RC. Search and clustering orders of magnitude faster than BLAST. *Bioinformatics* 2010;**26**:2460–1.

Edgar RC, Haas BJ, Clemente JC *et al.* UCHIME improves sensitivity and speed of chimera detection. *Bioinformatics* 2011;**27**:2194–200.

Englander L, Hull RJ. Reciprocal transfer of nutrients between ericaceous plants and a *Clavaria* sp. *New Phytologist* 1980;**84**:661–7.

Eskelinen A, Stark S, Mannisto M. Links between plant community composition, soil organic matter quality and microbial communities in contrasting tundra habitats. *Oecologia* 2009;**161**:113–23.

Euskirchen ES, Bret-Harte MS, Scott GJ *et al.* Seasonal patterns of carbon dioxide and water fluxes in three representative tundra ecosystems in northern Alaska. *Ecosphere* 2012;**3**:art4.

Fahnestock JT, Jones MH, Welker JM. Wintertime CO2 efflux from Arctic soils: Implications for annual carbon budgets. *Global Biogeochemical Cycles* 1999;**13**:775–9.

Frostegård A, Bååth E. The use of phospholipid fatty acid analysis to estimate bacterial and fungal biomass in soil. *Biology and Fertility of Soils* 1996;**22**:59–65.

Gadkari PS, McGuinness LR, Männistö MK *et al.* Arctic tundra soil bacterial communities active at subzero temperatures detected by stable isotope probing. *FEMS Microbiology Ecology* 2019;**96**, DOI: 10.1093/femsec/fiz192.

Gao D, Bai E, Yang Y *et al.* A global meta-analysis on freeze-thaw effects on soil carbon and phosphorus cycling. *Soil Biology and Biochemistry* 2021;**159**:108283.

Gavazov K, Ingrisch J, Hasibeder R *et al.* Winter ecology of a subalpine grassland: Effects of snow removal on soil respiration, microbial structure and function. *Science of The Total Environment* 2017;**590–591**:316–24.

Griffiths RI, Whiteley AS, O'Donnell AG *et al.* Rapid Method for Coextraction of DNA and RNA from Natural Environments for Analysis of Ribosomal DNA- and rRNA-Based Microbial Community Composition. *Applied and Environmental Microbiology* 2000;**66**:5488–91.

781 Groffman PM, Driscoll CT, Fahey TJ *et al.* Colder Soils in a Warmer World: A Snow Manipulation
782 Study in a Northern Hardwood Forest Ecosystem. *Biogeochemistry* 2001;**56**:135–50.
783 Grogan P, Jonasson S. Temperature and substrate controls on intra-annual variation in ecosystem
784 respiration in two subarctic vegetation types. *Global Change Biology* 2005;**11**:465–75.
785 Groisman PY, Knight RW, Easterling DR *et al.* Trends in Intense Precipitation in the Climate
786 Record. *Journal of Climate* 2005;**18**:1326–50.
787 Gtari M, Ghodhbane-Gtari F, Nouioui I *et al.* Phylogenetic perspectives of nitrogen-fixing
788 actinobacteria. *Archives of Microbiology* 2012;**194**:3–11.
789 Ihrmark K, Bödeker ITM, Cruz-Martinez K *et al.* New primers to amplify the fungal ITS2 region –
790 evaluation by 454-sequencing of artificial and natural communities. *FEMS Microbiology Ecology*
791 2012;**82**:666–77.
792 Jonasson S, Chapin FS, Shaver GR. 1.10 - Biogeochemistry in the Arctic: Patterns, Processes,
793 and Controls. In: Schulze E-D, Heimann M, Harrison S, et al. (eds.). *Global Biogeochemical*
794 *Cycles in the Climate System*. San Diego: Academic Press, 2001, 139–50.
795 Jonasson S, Michelsen A, Schmidt IK *et al.* Microbial biomass C, N and P in two arctic soils and
796 responses to addition of NPK fertilizer and sugar: implications for plant nutrient uptake.
797 *Oecologia* 1996;**106**:507–15.
798 Jonasson S, Michelsen A, Schmidt IK. Coupling of nutrient cycling and carbon dynamics in the
799 Arctic, integration of soil microbial and plant processes. *Applied Soil Ecology* 1999;**11**:135–46.
800 Kivinen S, Rasmus S, Jylhä K *et al.* Long-Term Climate Trends and Extreme Events in Northern
801 Fennoscandia (1914–2013). *Climate* 2017;**5**, DOI: 10.3390/cli5010016.
802 Kõljalg U, Nilsson RH, Abarenkov K *et al.* Towards a unified paradigm for sequence-based
803 identification of fungi. *Molecular Ecology* 2013;**22**:5271–7.
804 Lauber CL, Hamady M, Knight R *et al.* Pyrosequencing-Based Assessment of Soil pH as a
805 Predictor of Soil Bacterial Community Structure at the Continental Scale. *Applied and*
806 *Environmental Microbiology* 2009;**75**:5111–20.

807 Legendre P, Anderson MJ. Distance-based redundancy analysis: testing multispecies responses
808 in multifactorial ecological experiments. *Ecological Monographs* 1999;**69**:1–24.
809 Leopold DR. Ericoid fungal diversity: Challenges and opportunities for mycorrhizal research.
810 *Fungal Ecology* 2016;**24**:114–23.
811 Lépy É, Pasanen L. Observed Regional Climate Variability during the Last 50 Years in Reindeer
812 Herding Cooperatives of Finnish Fell Lapland. *Climate* 2017;**5**, DOI: 10.3390/cli5040081.
813 Li J, Mavrodi OV, Hou J *et al.* Comparative Analysis of Rhizosphere Microbiomes of Southern
814 Highbush Blueberry (Vaccinium corymbosum L.), Darrow's Blueberry (V. darrowii Camp), and
815 Rabbiteye Blueberry (V. virgatum Aiton). *Frontiers in Microbiology* 2020;**11**, DOI:
816 10.3389/fmicb.2020.00370.
817 Lorberau KE, Botnen SS, Mundra S *et al.* Does warming by open-top chambers induce change in
818 the root-associated fungal community of the arctic dwarf shrub Cassiope tetragona
819 (Ericaceae)? *Mycorrhiza* 2017;**27**:513–24.
820 Ma D, Yang G, Mu L *et al.* Tolerance of ectomycorrhizal fungus mycelium to low temperature and
821 freezing–thawing. *Canadian Journal of Microbiology* 2011;**57**:328–32.
822 Männistö M, Ganzert L, Tiirola M *et al.* Do shifts in life strategies explain microbial community
823 responses to increasing nitrogen in tundra soil? *Soil Biology and Biochemistry* 2016;**96**:216–28.
824 Männistö M, Vuosku J, Stark S *et al.* Bacterial and fungal communities in boreal forest soil are
825 insensitive to changes in snow cover conditions. *FEMS Microbiology Ecology* 2018;**94**, DOI:
826 10.1093/femsec/fiy123.
827 Männistö MK, Kurhela E, Tiirola M *et al.* Acidobacteria dominate the active bacterial communities
828 of Arctic tundra with widely divergent winter-time snow accumulation and soil temperatures.
829 *FEMS MicrobiolEcol* 2013;**84**:47–59.
830 Männistö MK, Tiirola M, Häggblom MM. Bacterial communities in Arctic fjelds of Finnish Lapland
831 are stable but highly pH-dependent. *FEMS MicrobiolEcol* 2007;**59**:452–65.

McCrystall MR, Stroeve J, Serreze M *et al.* New climate models reveal faster and larger increases in Arctic precipitation than previously projected. *Nature Communications* 2021;**12**:6765.

Mikan CJ, Schimel JP, Doyle AP. Temperature controls of microbial respiration in arctic tundra soils above and below freezing. *Soil Biology and Biochemistry* 2002;**34**:1785–95.

Mikkonen S, Laine M, Mäkelä HM *et al.* Trends in the average temperature in Finland, 1847–2013. *Stochastic Environmental Research and Risk Assessment* 2015;**29**:1521–9.

Mohagheghi A, Grohmann K, Himmel M *et al.* Isolation and Characterization of Acidothermus cellulolyticus gen. nov., sp. nov., a New Genus of Thermophilic, Acidophilic, Cellulolytic Bacteria. *International Journal of Systematic and Evolutionary Microbiology* 1986;**36**:435–43.

Morgado LN, Semenova TA, Welker JM *et al.* Long-term increase in snow depth leads to compositional changes in arctic ectomycorrhizal fungal communities. *Global Change Biology* 2016;**22**:3080–96.

Mundra S, Halvorsen R, Kauserud H *et al.* Ectomycorrhizal and saprotrophic fungi respond differently to long-term experimentally increased snow depth in the High Arctic. *MicrobiologyOpen* 2016;**5**:856–69.

Murphy J, Riley JP. A modified single solution method for the determination of phosphate in natural waters. *Analytica Chimica Acta* 1962;**27**:31–6.

Muyzer G, de Waal EC, Uitterlinden AG. Profiling of complex microbial populations by denaturing gradient gel electrophoresis analysis of polymerase chain reaction-amplified genes coding for 16S rRNA. *Appl Environ Microbiol* 1993;**59**:695–700.

Myers-Smith IH, Kerby JT, Phoenix GK *et al.* Complexity revealed in the greening of the Arctic. *Nature Climate Change* 2020;**10**:106–17.

Natali SM, Watts JD, Rogers BM *et al.* Large loss of CO2 in winter observed across the northern permafrost region. *Nature Climate Change* 2019;**9**:852–7.

Niittynen P, Heikkinen RK, Aalto J *et al.* Fine-scale tundra vegetation patterns are strongly related to winter thermal conditions. *Nature Climate Change* 2020;**10**:1143–8.

858 Nobrega S, Grogan P. Deeper Snow Enhances Winter Respiration from Both Plant-associated
859 and Bulk Soil Carbon Pools in Birch Hummock Tundra. *Ecosystems* 2007;**10**:419–31.
860 Oberwinkler F, Riess K, Bauer R *et al.* Enigmatic Sebacinales. *Mycological Progress* 2013;**12**:1–
861 27.
862 Oechel WC, Vourlitis G, Hastings SJ. Cold season CO2 emission from Arctic soils. *Global*
863 *Biogeochemical Cycles* 1997;**11**:163–72.
864 Oksanen L, Virtanen R. Topographic, altitudinal and regional patterns in continental and
865 suboceanic heath vegetation of northern Fennoscandia. *Acta. Bot. Fennica* 1995; **153**:1-80.
866 Olofsson J, Oksanen L, Callaghan T *et al.* Herbivores inhibit climate-driven shrub expansion on
867 the tundra. *Global Change Biology* 2009;**15**:2681–93.
868 Olsson PA. Signature fatty acids provide tools for determination of the distribution and interactions
869 of mycorrhizal fungi in soil. *FEMS Microbiology Ecology* 1999;**29**:303–10.
870 Pattison, RR, Welker JM. Differential ecophysiological response of deciduous shrubs and a
871 graminoid to long-term experimental snow reductions and additions in moist acidic tundra,
872 Northern Alaska. *Oecologia* 2014; **174**, 339–350. https://doi.org/10.1007/s00442-013-2777-6
873 Perez-Mon C, Frey B, Frossard A. Functional and Structural Responses of Arctic and Alpine Soil
874 Prokaryotic and Fungal Communities Under Freeze-Thaw Cycles of Different Frequencies.
875 *Frontiers in Microbiology* 2020;**11**, DOI: 10.3389/fmicb.2020.00982.
876 Pessi IS, Viitamäki S, Virkkala A-M *et al.* In-depth characterization of denitrifier communities
877 across different soil ecosystems in the tundra. *Environmental Microbiome* 2022;**17**:30.
878 Price MN, Dehal PS, Arkin AP. FastTree: Computing Large Minimum Evolution Trees with Profiles
879 instead of a Distance Matrix. *Molecular Biology and Evolution* 2009;**26**:1641–50.
880 Quast C, Pruesse E, Yilmaz P *et al.* The SILVA ribosomal RNA gene database project: improved
881 data processing and web-based tools. *Nucleic Acids Research* 2012;**41**:D590–6.
882 Rantanen M, Karpechko AYu, Lipponen A *et al.* The Arctic has warmed nearly four times faster
883 than the globe since 1979. *Communications Earth & Environment* 2022;**3**:168.

884 Ricketts MP, Matamala R, Jastrow JD *et al.* The effects of warming and soil chemistry on bacterial
885 community structure in Arctic tundra soils. *Soil Biology and Biochemistry* 2020;**148**:107882.
886 Ricketts MP, Poretsky RS, Welker JM *et al.* Soil bacterial community and functional shifts in
887 response to altered snowpack in moist acidic tundra of northern Alaska. *SOIL* 2016;**2**:459–74.
888 Rixen C, Høye TT, Macek P *et al.* Winters are changing: snow effects on Arctic and alpine tundra
889 ecosystems. *Arctic Science* 2022;**8**:572–608.
890 Ruess L, Häggblom MM, Zapata EJG *et al.* Fatty acids of fungi and nematodes—possible
891 biomarkers in the soil food chain? *Soil Biology and Biochemistry* 2002;**34**:745–56.
892 Schimel JP, Bennett J. Nitrogen mineralization: challenges of a changing paradigm. *Ecology*
893 2004;**85**:591–602.
894 Schimel JP, Bilbrough C, Welker JM. Increased snow depth affects microbial activity and nitrogen
895 mineralization in two Arctic tundra communities. *Soil Biology and Biochemistry* 2004;**36**:217–27.
896 Schuur EAG, McGuire AD, Schädel C *et al.* Climate change and the permafrost carbon feedback.
897 *Nature* 2015;**520**:171–9.
898 Selosse M-A, Setaro S, Glatard F *et al.* Sebacinales are common mycorrhizal associates of
899 Ericaceae. *New Phytol* 2007;**174**:864–78.
900 Semenchuk PR, Christiansen CT, Grogan P *et al.* Long-term experimentally deepened snow
901 decreases growing-season respiration in a low- and high-arctic tundra ecosystem. *Journal of*
902 *Geophysical Research: Biogeosciences* 2016;**121**:1236–48.
903 Semenova TA, Morgado LN, Welker JM *et al.* Compositional and functional shifts in arctic fungal
904 communities in response to experimentally increased snow depth. *Soil Biology and*
905 *Biochemistry* 2016;**100**:201–9.
906 Serreze MC, Gustafson J, Barrett AP *et al.* Arctic rain on snow events: bridging observations to
907 understand environmental and livelihood impacts. *Environmental Research Letters*
908 2021;**16**:105009.

Stark S, Eskelinen A, Männistö MK. Regulation of Microbial Community Composition and Activity by Soil Nutrient Availability, Soil pH, and Herbivory in the Tundra. *Ecosystems* 2012;**15**:18–33.

Stark S, Kumar M, Myrsky E *et al.* Decreased Soil Microbial Nitrogen Under Vegetation 'Shrubification' in the Subarctic Forest–Tundra Ecotone: The Potential Role of Increasing Nutrient Competition Between Plants and Soil Microorganisms. *Ecosystems* 2023, DOI: 10.1007/s10021-023-00847-z.

Stark S, Kytöviita M-M. Simulated grazer effects on microbial respiration in a subarctic meadow: Implications for nutrient competition between plants and soil microorganisms. *Applied Soil Ecology* 2006;**31**:20–31.

Stark S, Väisänen M. Insensitivity of Soil Microbial Activity to Temporal Variation in Soil N in Subarctic Tundra: Evidence from Responses to Large Migratory Grazers. *Ecosystems* 2014;**17**:906–17.

Sturm M, Holmgren J, McFadden JP *et al.* Snow–Shrub Interactions in Arctic Tundra: A Hypothesis with Climatic Implications. *Journal of Climate* 2001a;**14**:336–44.

Sturm M, Racine C, Tape K. Increasing shrub abundance in the Arctic. *Nature* 2001b;**411**:546–7.

Sturm M, Schimel J, Michaelson G *et al.* Winter Biological Processes Could Help Convert Arctic Tundra to Shrubland. *BioScience* 2005;**55**:17–26.

Sullivan PF, Stokes MC, McMillan CK *et al.* Labile carbon limits late winter microbial activity near Arctic treeline. *Nature Communications* 2020;**11**:4024.

Sullivan PF, Welker JM, Arens SJT *et al.* Continuous estimates of CO2 efflux from arctic and boreal soils during the snow-covered season in Alaska. *Journal of Geophysical Research: Biogeosciences* 2008;**113**, DOI: https://doi.org/10.1029/2008JG000715.

Tao X, Feng J, Yang Y *et al.* Winter warming in Alaska accelerates lignin decomposition contributed by Proteobacteria. *Microbiome* 2020;**8**:84.

933 Tarnocai C, Canadell JG, Schuur EAG *et al.* Soil organic carbon pools in the northern circumpolar
934 permafrost region. *Global Biogeochemical Cycles* 2009;**23**, DOI:
935 https://doi.org/10.1029/2008GB003327.
936 Tedersoo L, Bahram M, Põlme S *et al.* Global diversity and geography of soil fungi. *Science*
937 2014;**346**:1256688.
938 Tilston EL, Sparrman T, Öquist MG. Unfrozen water content moderates temperature dependence
939 of sub-zero microbial respiration. *Soil Biology and Biochemistry* 2010;**42**:1396–407.
940 Timonen S, Sinkko H, Sun H *et al.* Ericoid Roots and Mycospheres Govern Plant-Specific
941 Bacterial Communities in Boreal Forest Humus. *Microb Ecol* 2017;**73**:939–53.
942 Tsoy OV, Ravcheev DA, Čuklina J *et al.* Nitrogen Fixation and Molecular Oxygen: Comparative
943 Genomic Reconstruction of Transcription Regulation in Alphaproteobacteria. *Frontiers in*
944 *Microbiology* 2016;**7**, DOI: 10.3389/fmicb.2016.01343.
945 Viitamäki S, Pessi IS, Virkkala A-M *et al.* The activity and functions of soil microbial communities in
946 the Finnish sub-Arctic vary across vegetation types. *FEMS Microbiology Ecology* 2022;**98**, DOI:
947 10.1093/femsec/fiac079.
948 Vohník M, Pánek M, Fehrer J *et al.* Experimental evidence of ericoid mycorrhizal potential within
949 Serendipitaceae (Sebacinales). *Mycorrhiza* 2016;**26**:831–46.
950 Voříšková J, Elberling B, Priemé A. Fast response of fungal and prokaryotic communities to
951 climate change manipulation in two contrasting tundra soils. *Environmental Microbiome*
952 2019;**14**:6.
953 Vowles T, Björk RG. Implications of evergreen shrub expansion in the Arctic. *Journal of Ecology*
954 2019;**107**:650–5.
955 Wallenstein MD, McMahon S, Schimel JP. Seasonal variation in enzyme activities and
956 temperature sensitivities in Arctic tundra soils. *Global Change Biology* 2009;**15**.

957 Wang Q, Garrity GM, Tiedje JM *et al.* Naïve Bayesian Classifier for Rapid Assignment of rRNA
958 Sequences into the New Bacterial Taxonomy. *Applied and Environmental Microbiology*
959 2007;**73**:5261–7.
960 Way RG, Lewkowicz AG. Environmental controls on ground temperature and permafrost in
961 Labrador, northeast Canada. *Permafrost and Periglac Process*. 2018; **29**: 73–85.
962 Weintraub MN, Schimel JP. Seasonal protein dynamics in Alaskan arctic tundra soils. *Soil Biology*
963 *and Biochemistry* 2005a;**37**:1469–75.
964 Weintraub MN, Schimel JP. The seasonal dynamics of amino acids and other nutrients in Alaskan
965 Arctic tundra soils. *Biogeochemistry* 2005b;**73**:359–80.
966 Weiß M, Waller F, Zuccaro A *et al.* Sebacinales – one thousand and one interactions with land
967 plants. *New Phytologist* 2016;**211**:20–40.
968 Yang H, Zhao X, Liu C *et al.* Diversity and characteristics of colonization of root-associated fungi
969 of Vaccinium uliginosum. *Scientific Reports* 2018;**8**:15283.
970

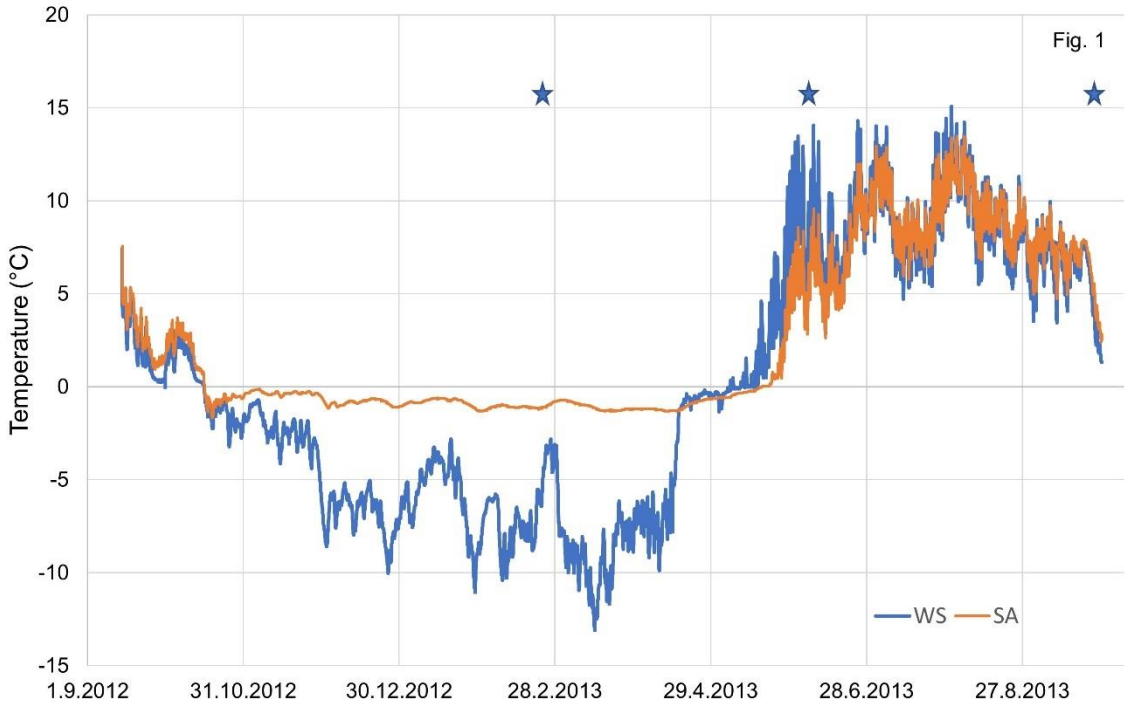

Figure 1. Soil temperature in the windswept and snow accumulating tundra heaths. Values are means obtained by data loggers in each plot (N=4). Stars denote the sampling points for bacterial and fungal community analyses.

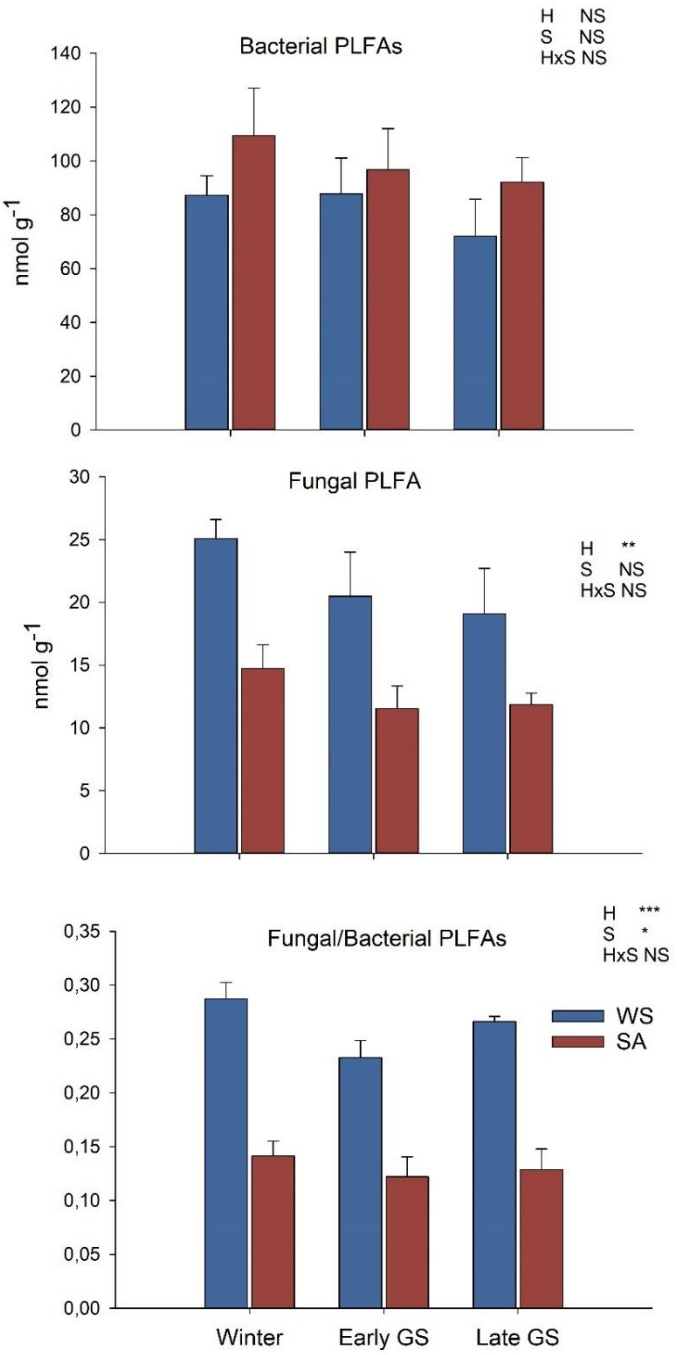

Figure 2. Bacterial and fungal PLFAs and their ratio in windswept and snow accumulating tundra heaths sampled in winter, early and late growing season. Values are means ± S.E., N=4. Significant differences of between the habitats (H) or sampling season (S) were analyzed using linear mixed effect model (Supplementary Table S1). Significance levels: ***, $p<0.001$; **, $p<0.01$; *, $p<0.05$; NS, not significant.

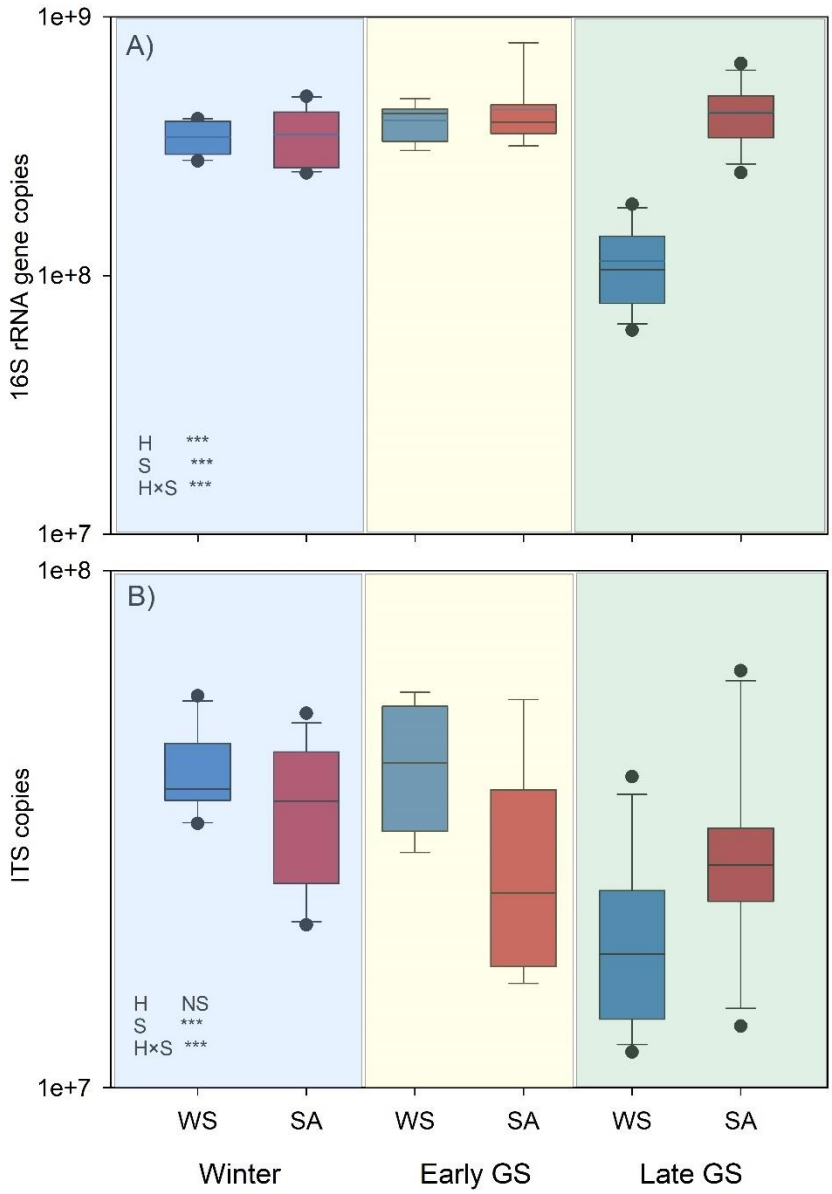

Figure 3. Bacterial 16S rRNA and fungal ITS copy numbers in windswept and snow accumulating tundra heaths sampled in winter, early and late growing season. Values are means ± S.E., N=4. Significant differences of between the habitats (H) or sampling season (S) were analyzed using linear mixed effect model (Supplementary Table S1). Significance levels: ***, $p<0.001$; **, $p<0.01$; *, $p<0.05$; NS, not significant.

Fig. 4

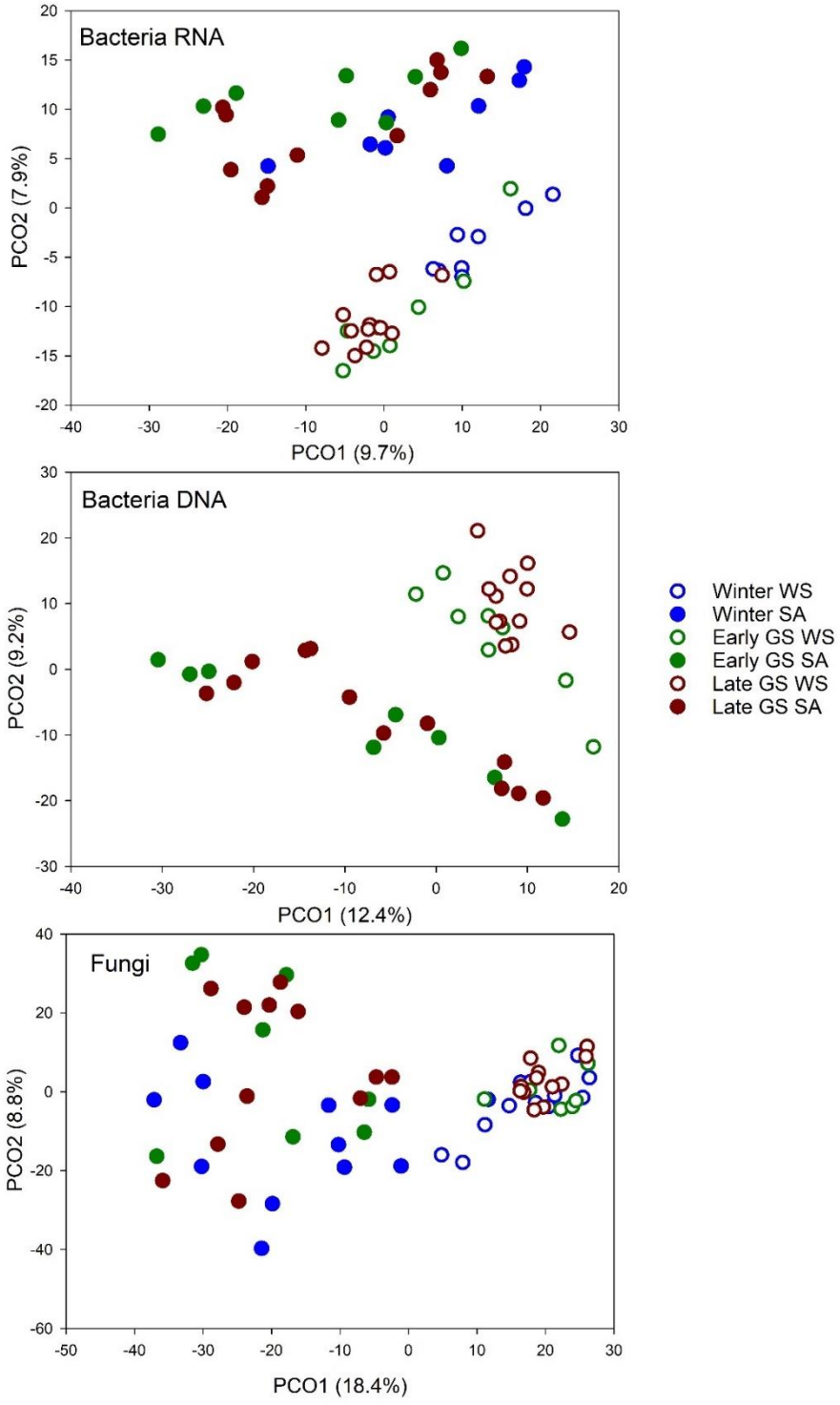

Figure 4. PCO ordination of active (RNA derived) and total (DNA derived) bacterial communities and total fungal communities in windswept and snow accumulating tundra heaths. Winter DNA derived bacterial communities are excluded from the ordination due to possible technological bias in the data (see Materials and Methods).

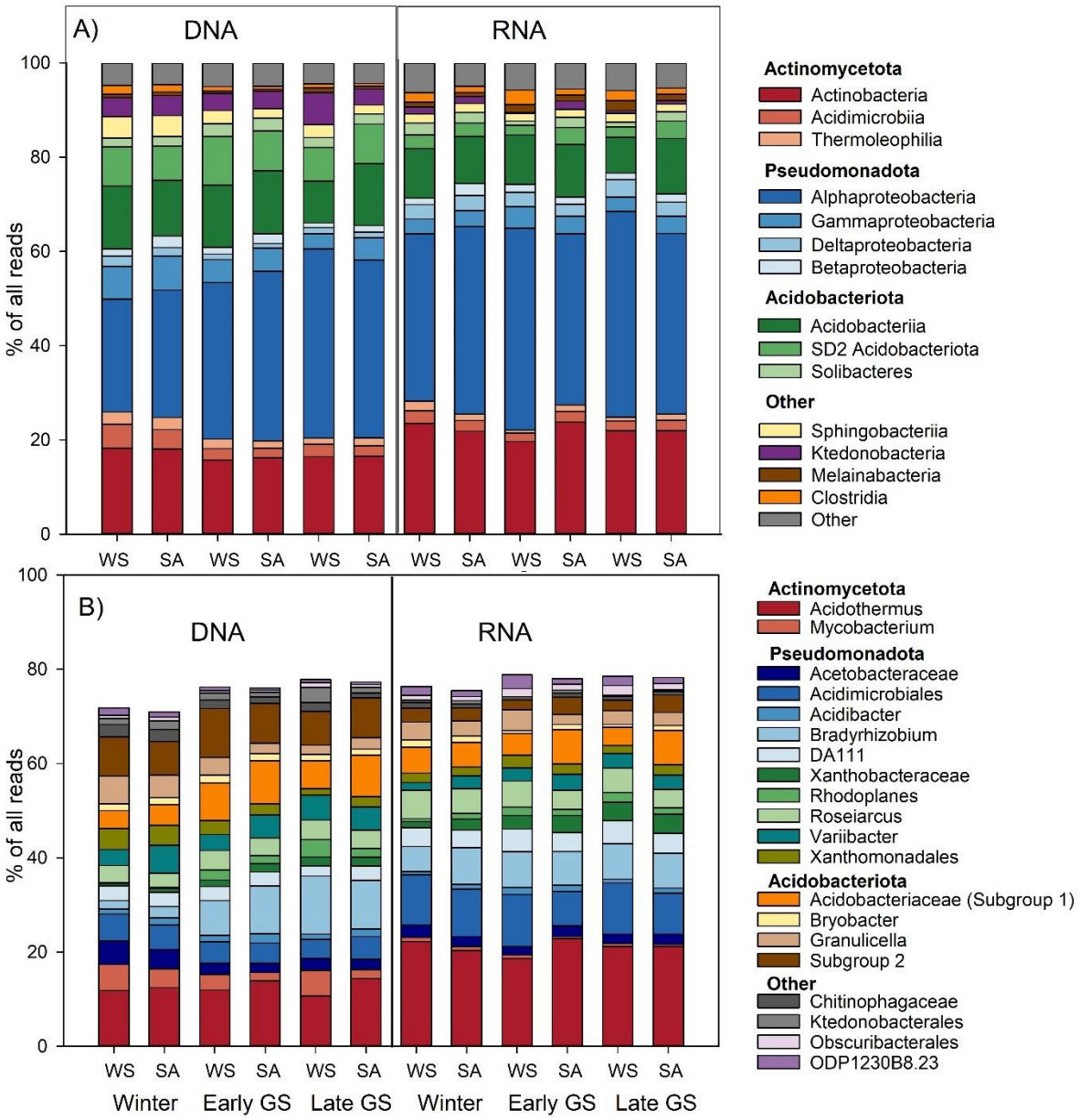

Figure 5. Abundance of bacterial classes (A) and dominant genera (B) in windswept and snow accumulating tundra heaths sampled in winter, early and late growing season.

Fig 6.

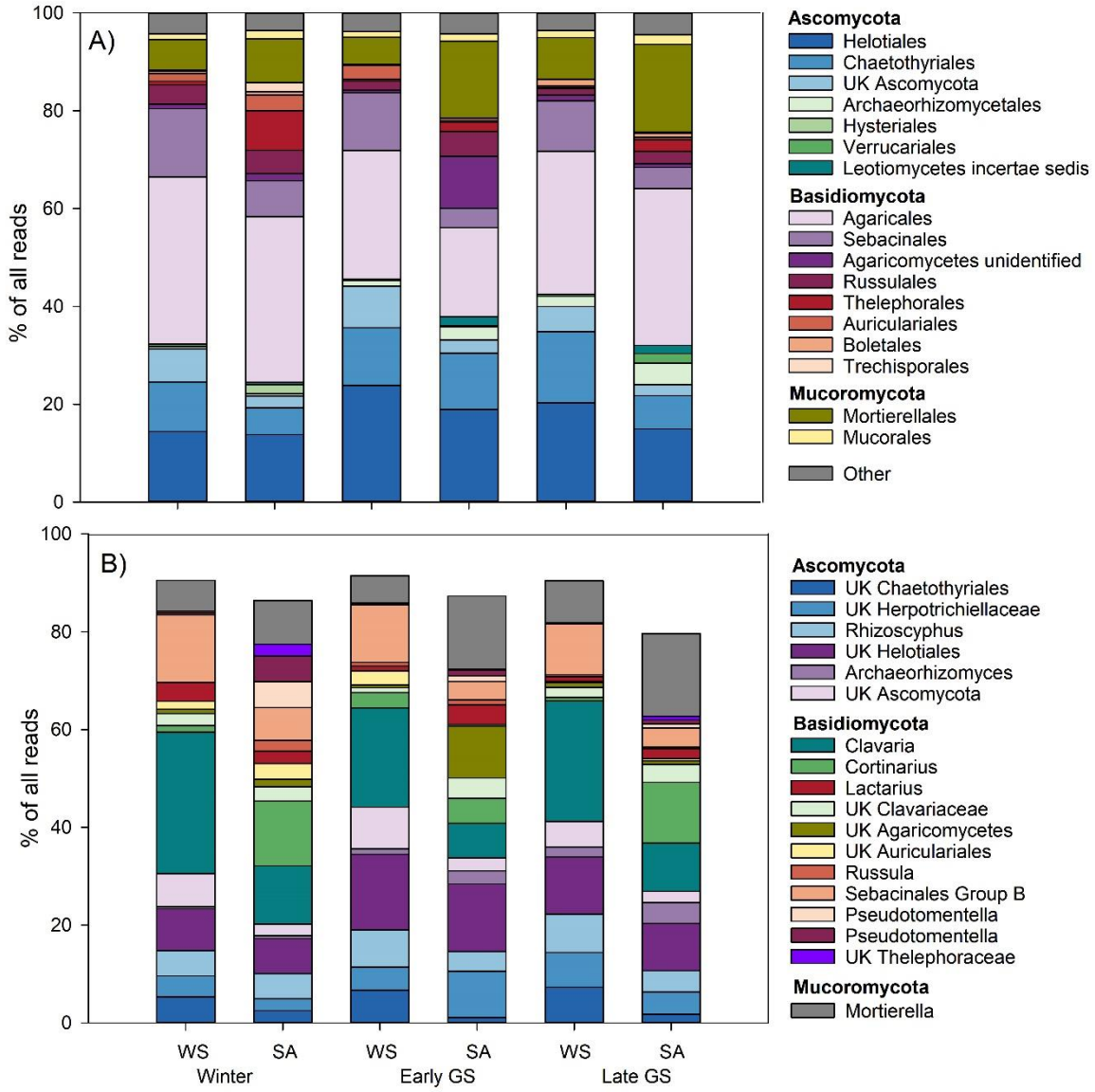

Figure 6. Abundance of fungal orders (A) and dominant genera (B) in windswept and snow accumulating tundra heaths sampled in winter, early and late growing season. UK=unknown.

Table 1. Soil physicochemical properties in windswept (WS) and snow accumulating (SA) tundra heaths.

Values are means with S.E. in brackets.

	Winter		Early GS		Late GS	
	WS	SA	WS	SA	WS	SA
pH	4.6 (0.04)	4.5 (0.03)	4.7 (0.04)	4.6 (0.04)	4.6 (0.03)	4.4 (0.07)
OM (%)	75.4 (4.7)	68.1 (6.5)	74.2 (5.0)	69.4 (3.1)	73.6 (5.5)	69.0 (4.2)
DW (%)	35.1 (2.5)	37.2 (2.6)	36.1 (2.4)	32.0 (1.2)	32.6 (2.4)	32.4 (1.7)
N_{tot} ($mgkg^{-1}$)	45.9 (3.1)	94.4 (10.0)	53.8 (2.4)	100.4 (15.3)	32.9 (1.5)	81.3 (6.7)
N_{org} ($mgkg^{-1}$)	43.9 (3.0)	78.1 (7.8)	50.1 (2.3)	90.9 (13.0)	30.8 (1.4)	74.8 (5.6)
NO_3 ($mgkg^{-1}$)	0.25 (0.02)	0.47 (0.08)	0.16 (0.01)	0.26 (0.02)	0.27 (0.02)	0.19 (0.05)
NH_4 ($mgkg^{-1}$)	1.74 (0.13)	15.82 (6.0)	3.53 (0.26)	9.18 (2.3)	1.82 (0.26)	6.33 (1.2)
N_{mic} ($mgkg^{-1}$)	158.4 (11.7)	129.3 (8.4)	130.4 (12.5)	93.8 (6.4)	125.0 (5.1)	92.1 (6.0)
P_{tot} ($mgkg^{-1}$)	15.1 (1.9)	52.8 (14.3)	13.3 (1.8)	43.2 (4.6)	10.0 (0.83)	32.3 (8.7)
P_{mic}($mgkg^{-1}$)	76.4 (9.9)	58.8 (11.7)	48.5 (11.7)	51.4 (5.7)	45.5 (5.6)	41.5 (8.2)

Table 2. PERMANOVA main test for bacterial (derived from RNA and DNA) and fungal community structure in windswept and snow accumulating habitats (Ha) across three different seasons (Se) in four plots per habitat. Significance levels: $p<0.05$ are underlined, $p<0.01$ are indicated by bold

Source of variation	SS	MS	Pseudo-F	P (perm)	Variance explained (%)
Bacteria RNA					
Habitat	4726	4726,4	2,33	**0,01**	14,6
Season	5032	2516,1	2,40	**0,001**	12,8
Plot(Ha)	14865	2123,5	2,02	**0,001**	18,5
Se×Ha	2955	1477,6	1,41	**0,001**	9,8
Bacteria DNA[a]					
Habitat	4903	4902,7	2,43	0,018	17,5
Season	1613	1613,1	1,57	**0,001**	8,2
Plot(Ha)	14460	2065,7	2,02	**0,001**	21,6
Se×Ha	1331	1331,4	1,30	0,047	8,4
Fungi DNA					
Habitat	19501	19501	4,15	**0,002**	21,5
Season	7428	3713,7	2,30	**0,001**	9,7
Plot(Ha)	34990	4998,6	3,10	**0,001**	20,7
Se×Ha	5969	2984,4	1,85	**0,001**	11,1

[a] For the bacterial DNA PERMANOVA analyses, only samples from early and late growing season were included.

Supplementary Figures

Figure S1. Pictures of the field site: North side of Mt Pikku-Malla showing windswept ridges and snow accumulating depressions (A), sampling of deep snow (B) and windswept (C) plots, vegetation of snow accumulating (D) and windswept (E) plots, field site in winter (F) and summer (G)

Figure S2. PCO ordination of active (RNA derived) and total (DNA derived) bacterial communities in WS and SA tundra heaths sampled in winter, early and late growing season showing the separation of the winter DNA derived community from all other sampling seasons. Abbreviations: D=DNA, R=RNA, WS=windswept, SA=snow accumulating, EGS=early growing season, LGS=late growing season.

Figure S3. PCO ordination and relative abundance of bacterial genera in the DNA and RNA derived bacterial communities of WS and SA tundra heaths. Winter DNA samples are excluded from the PCO ordination. Abbreviations: D=DNA, R=RNA, WS=windswept, SA=snow accumulating, EGS=early growing season, LGS=late growing season.

Figure S4. Abundance of the ten most dominating bacterial genera in RNA samples from windswept and snow-accumulating tundra heaths sampled in winter (Feb), early growing season (June) or late growing season (Sept). Significant effects of habitat, season or their interactions were tested using PERMANOVA. Significance levels ***, $p<0.001$; **, $p<0.01$; *, $p<0.05$; NS, not significant.

Figure S5. Abundance of the ten most dominating fungal genera in RNA samples from windswept and snow-accumulating tundra heaths sampled in winter (Feb), early growing season (June) or late growing season (Sept). Significant effects of habitat, season or their interactions were tested using PERMANOVA. Significance levels ***, $p<0.001$; **, $p<0.01$; *, $p<0.05$; NS, not significant.

Figure S6. Figure S6. Distance based redundancy analysis plots showing the best predictors in the DistLM model explaining active bacterial (A), total bacterial (B) and fungal (C) community structure.

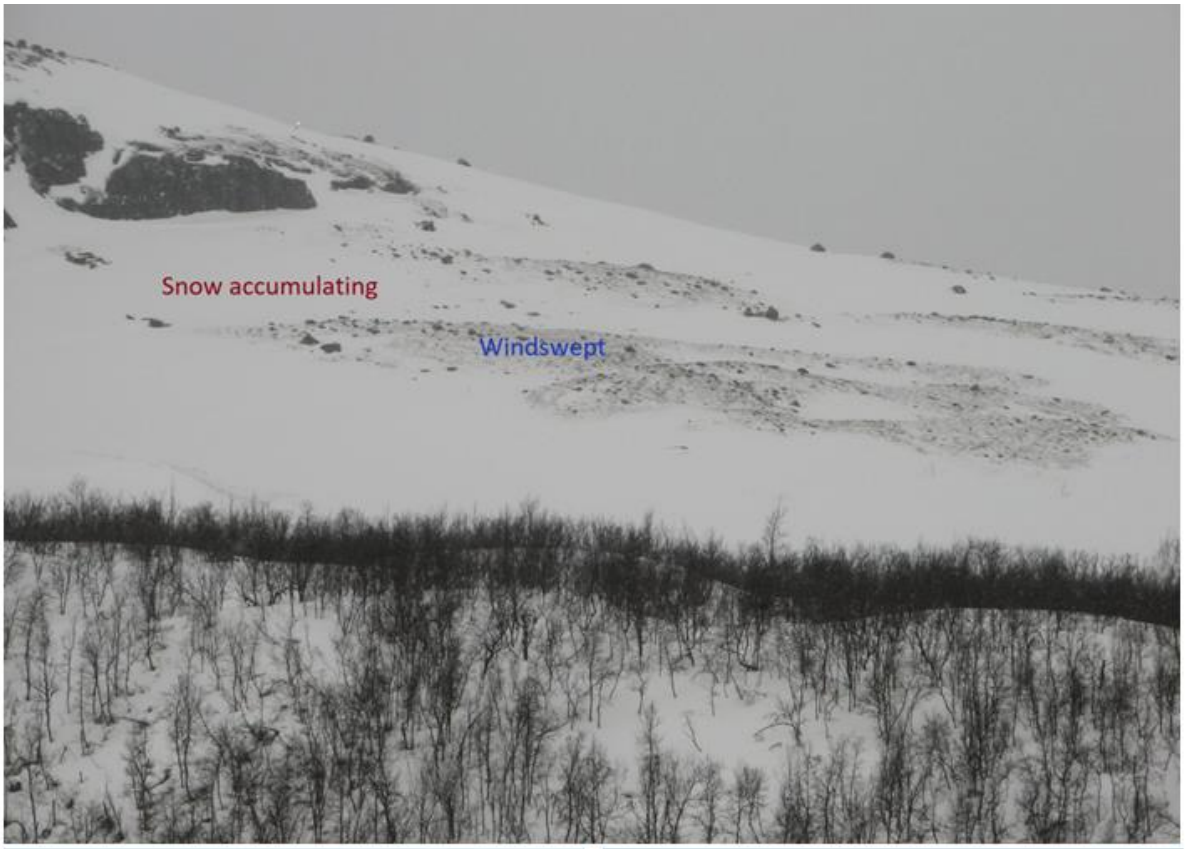
Snow accumulating
Windswept

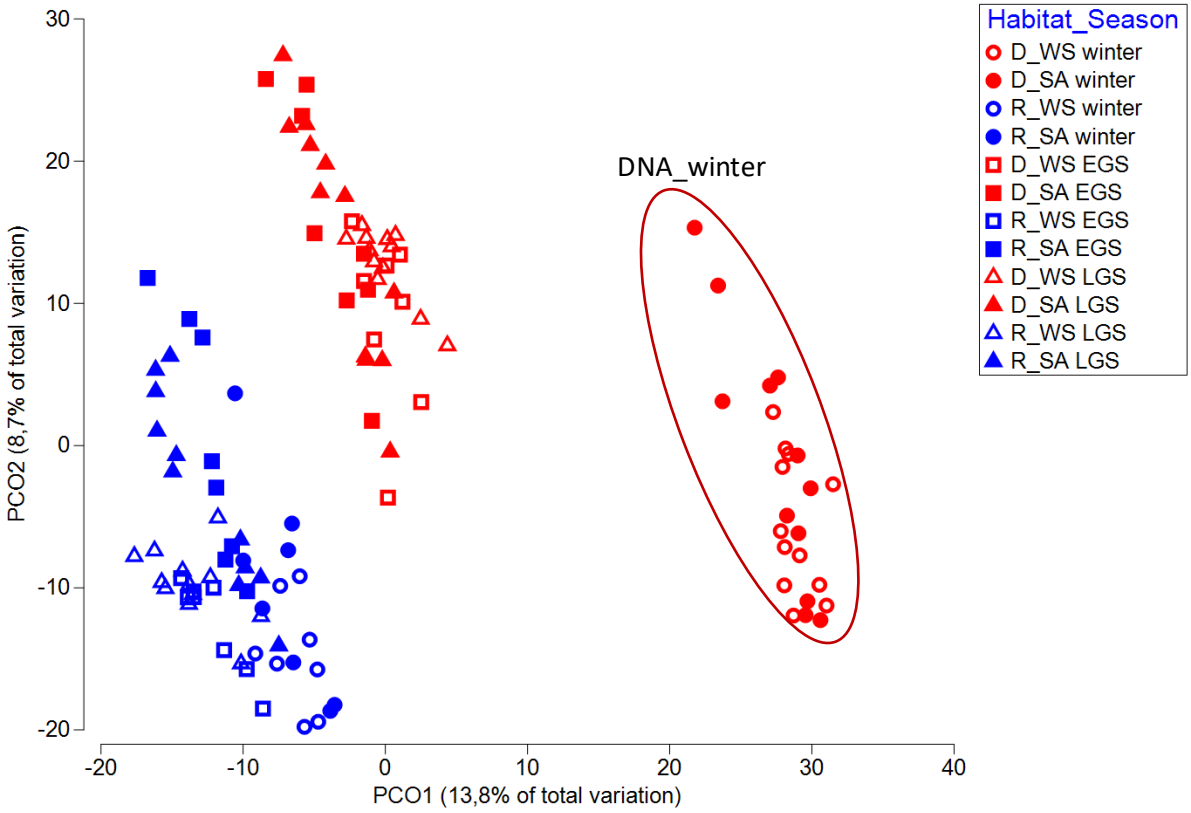

Supplementary Figure S2. PCO ordination of active (RNA derived) and total (DNA derived) bacterial communities in WS and SA tundra heaths sampled in winter, early and late growing season showing the separation of the winter DNA derived community from all other sampling seasons. Abbreviations: D=DNA, R=RNA, WS=windswept, SA=snow accumulating, EGS=early growing season, LGS=late growing season.

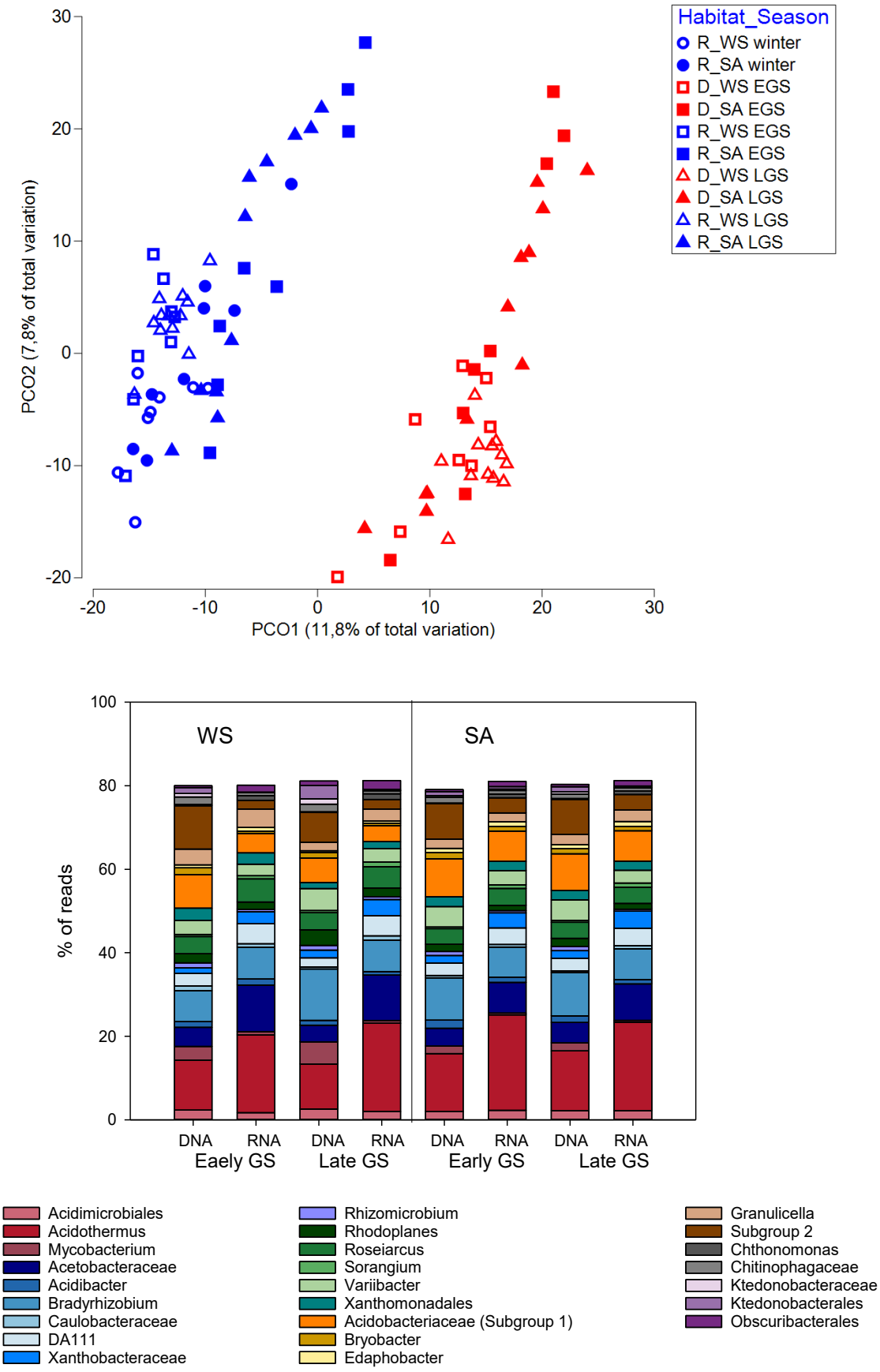

Supplementary Figure S3. PCO ordination and relative abundance of bacterial genera in the DNA and RNA derived bacterial communities of WS and SA tundra heaths. Winter DNA samples are excluded from the PCO ordination. Abbreviations: D=DNA, R=RNA, WS=windswept, SA=snow accumulating, EGS=early growing season, LGS=late growing season.

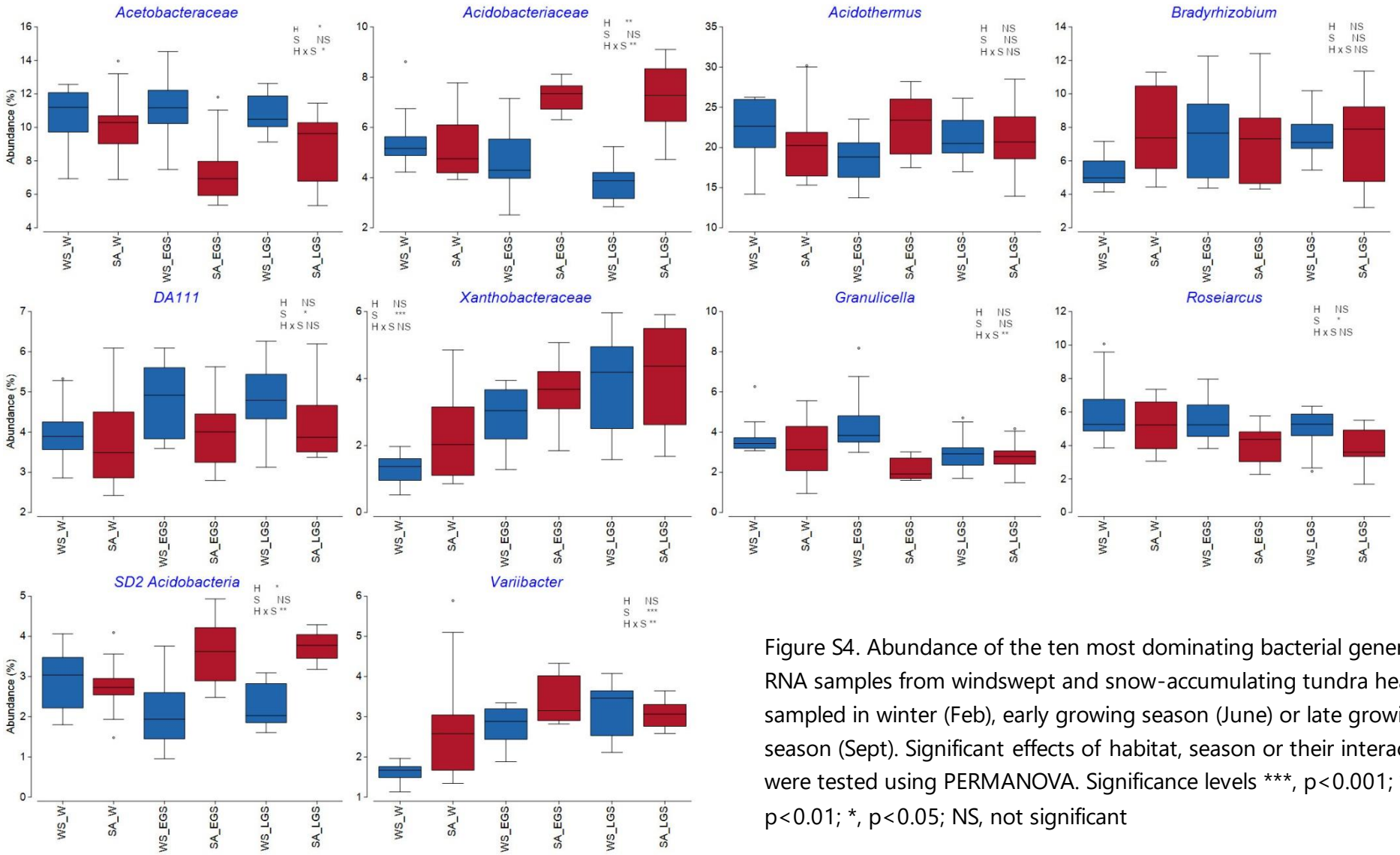

Figure S4. Abundance of the ten most dominating bacterial genera in RNA samples from windswept and snow-accumulating tundra heaths sampled in winter (Feb), early growing season (June) or late growing season (Sept). Significant effects of habitat, season or their interactions were tested using PERMANOVA. Significance levels ***, $p<0.001$; **, $p<0.01$; *, $p<0.05$; NS, not significant

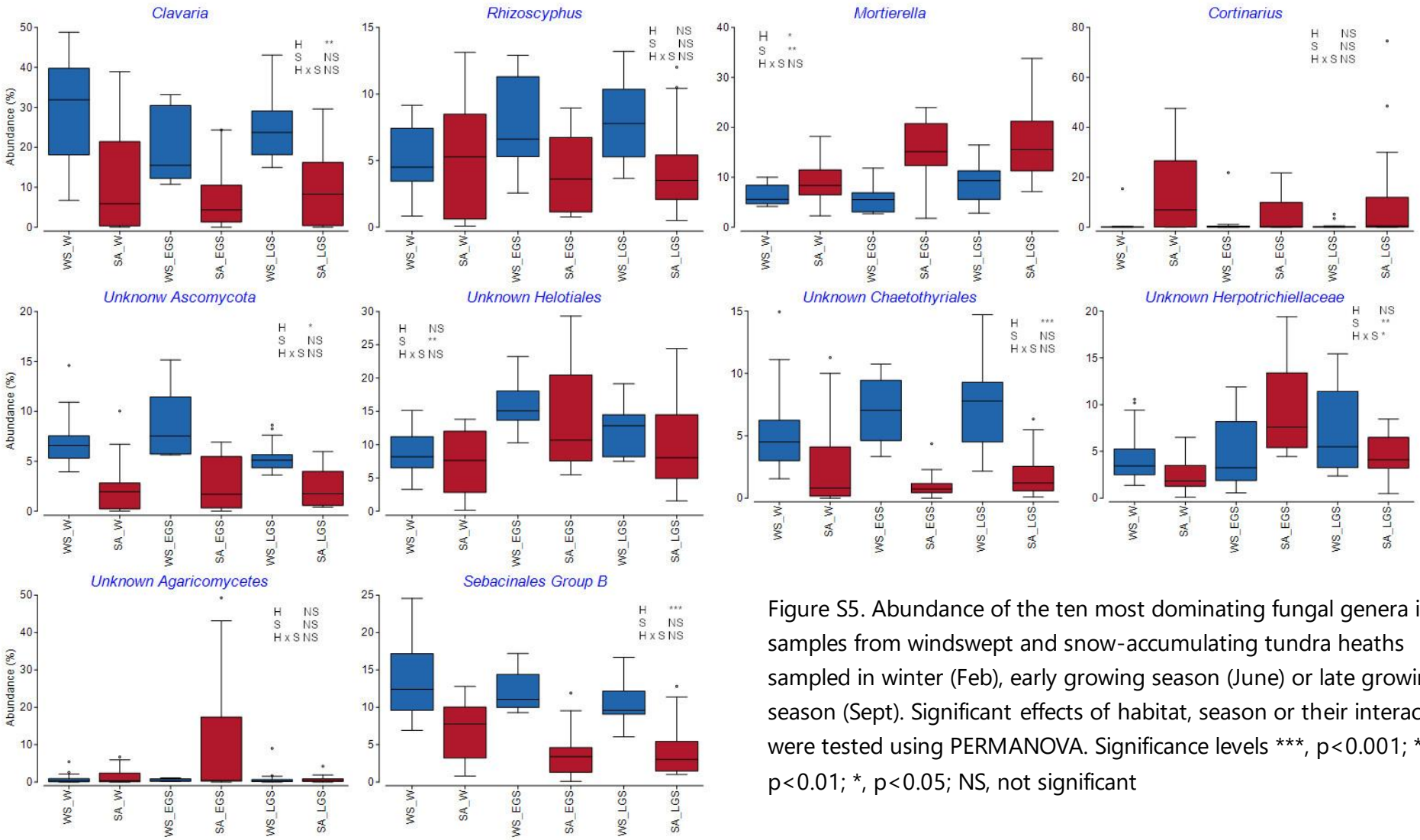

Figure S5. Abundance of the ten most dominating fungal genera in RNA samples from windswept and snow-accumulating tundra heaths sampled in winter (Feb), early growing season (June) or late growing season (Sept). Significant effects of habitat, season or their interactions were tested using PERMANOVA. Significance levels ***, $p<0.001$; **, $p<0.01$; *, $p<0.05$; NS, not significant

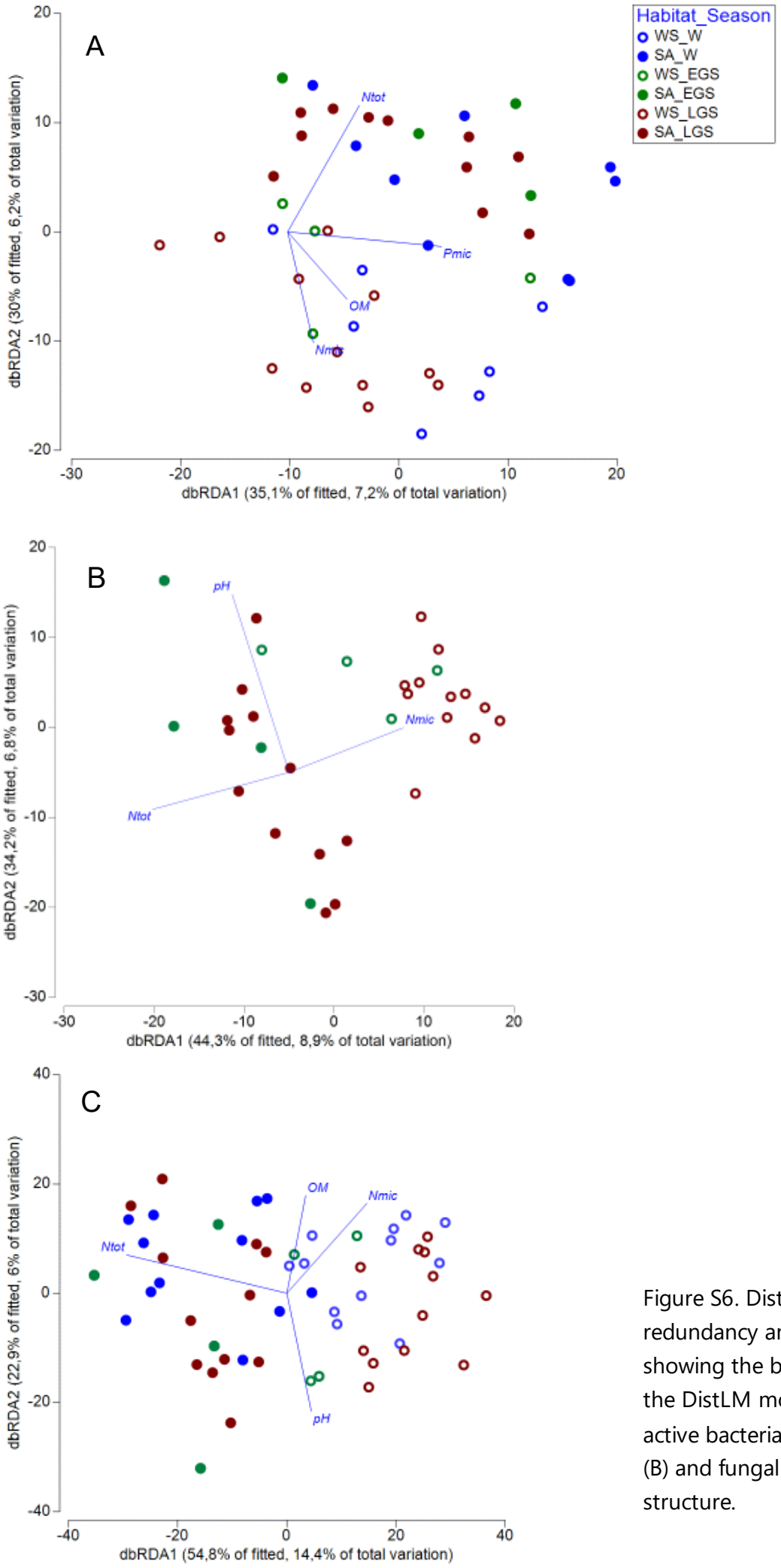

Figure S6. Distance based redundancy analysis plots showing the best predictors in the DistLM model explaining active bacterial (A), total bacterial (B) and fungal (C) community structure.